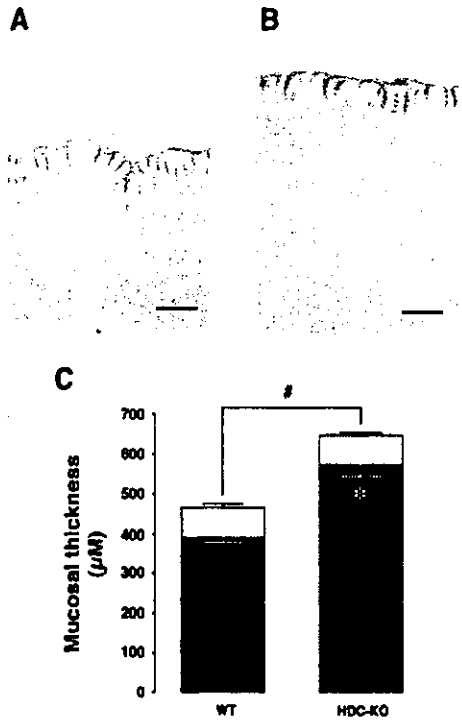

Fig. 3. Periodic acid Schiff staining of the gastric mucosa of 6-mo-old WT (*A*) and HDC-KO (*B*) mice (bar = 100 μm). Thickness of the oxyntic mucosa, pit region (open column; presence of surface mucous cells), and glandular basal region (filled column; presence of parietal, chief, and endocrine cells) in WT and HDC-KO mice (*C*). Note that the change in gastric mucosal thickness was most prominent in the glandular basal region compared with the pit region. Values are means ± SE, n = 7. Significant differences in the #mucosal thickness and *glandular base region for HDC-KO mice compared with WT mice ($P < 0.05$).

mice compared with H_2R-KO mice (29, 44). Because there have been reports that other histamine receptors, i.e., H_1R (16, 38, 39) and H_3R (40), possess the potential to positively modulate gastric mucosal proliferation, it remains possible that histamine receptor signals might affect gastric mucosal hyperplasia in different manners. For instance, H_1R and H_3R might relate to promote hyperplasia, whereas H_2R relates to inhibit hyperplasia. This explanation could account for the mild hyperplastic mucosa and absence of albumin loss from the gastric mucosa observed in HDC-KO mice. In addition, the difference between the ligand and receptor deficiency, i.e., the observation that, whereas HDC-KO mice decreased basal acid secretion with increased intragastric pH (52), H_2R-KO mice have normal basal acid secretion (29, 44), would also support the explanation that other histamine receptors are involved in gastric mucosal functions.

In rodent gastric mucosa, ECL and mast cells represent the major histamine-producing cell (25, 46). Pharmacological analysis with α-FMH, which preferentially inhibits histamine synthesis in ECL cells, demonstrated that ECL cell-derived histamine predominantly regulates gastric acid secretion (2, 3, 5, 10, 13, 43) and mucosal morphology (2, 3, 5, 10, 13, 37). It has already been reported with different strains of mast cell-deficient mice, such as *W/W*^{v} (49) and C57B1/6J-*mi/mi* (50), that mast cells partially contribute to gastric acid secretion. Nonetheless, the role of mast cells for regulation of gastric mucosal morphology remains uncertain. The present study confirmed that gastric mucosal histamine levels in *W/W*^{v} mice were half the levels measured in +/+ mice, with no difference observed for intragastric pH and serum gastrin levels between the two groups. Similarly, gastric oxyntic mucosal morphology was normal in *W/W*^{v} mice even 1 yr after birth. These results indicate that mast cell-derived histamine does not play a critical role for maintenance of gastric mucosal architecture, probably due to presence of ECL-derived histamine.

To detect ECL cells with immunohistochemical analysis, anti-Cg A antibody was used instead of anti-HDC and anti-

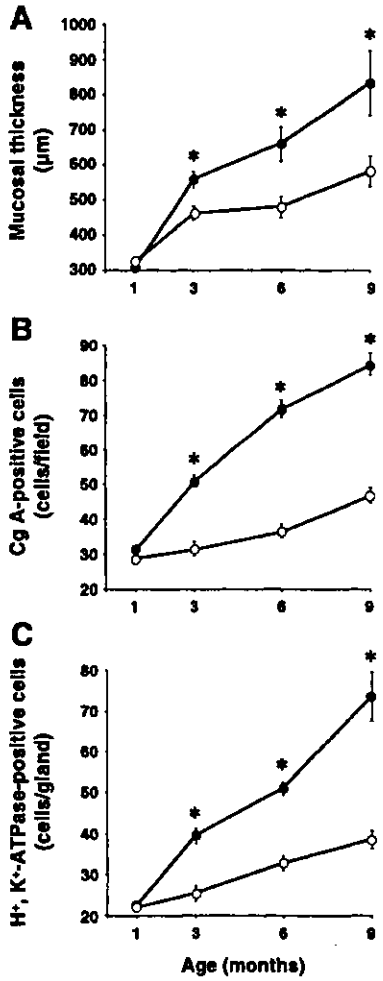

Fig. 4. Time-course comparison of oxyntic mucosal thickness (*A*) and both chromogranin A (Cg A)-positive endocrine (*B*) and parietal cell counts (*C*) in WT (open circles) and HDC-KO (closed circles) mice. Sections were evaluated with hematoxylin and eosin staining (*A*) and immunostaining. Three months after birth, all 3 parameters in HDC-KO mice were significantly increased compared with WT mice. Values are means ± SE, n = 6–8. *Significant differences from WT mice of the same age ($P < 0.05$.)

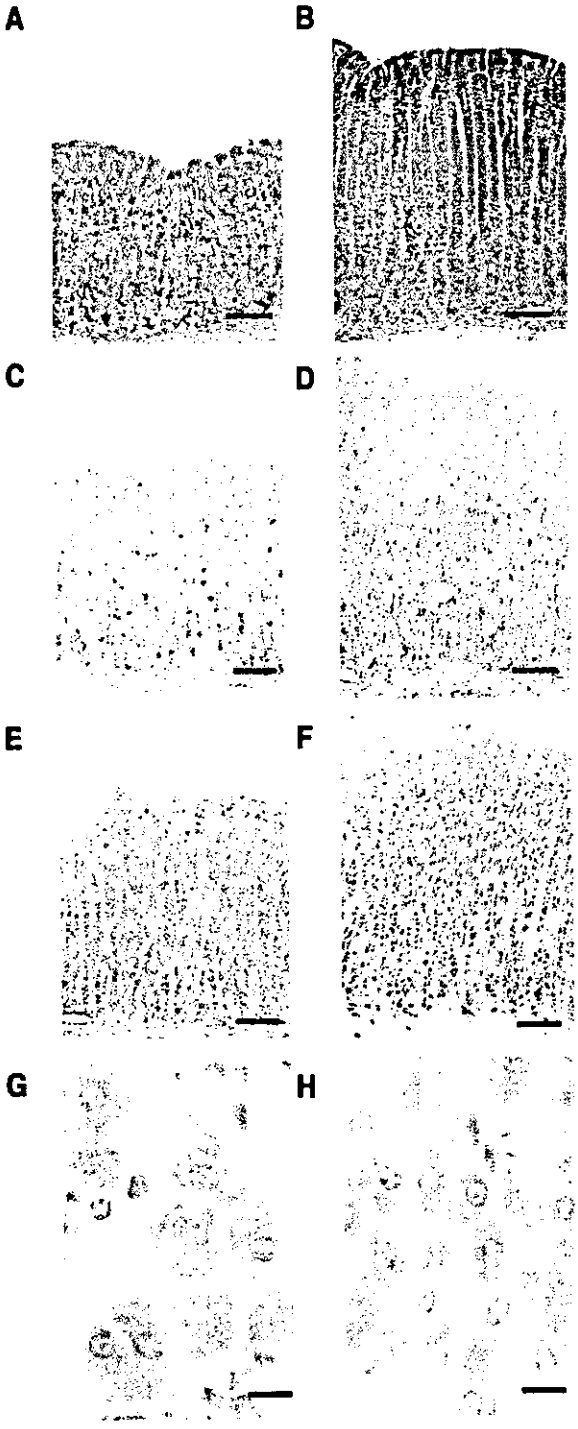

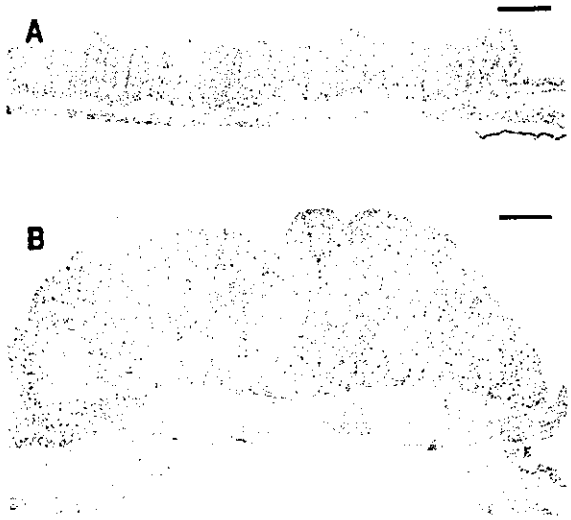

Fig. 6. Immunohistochemical staining of gastric oxyntic mucosa with Cg A antibody in 9-mo-old WT (*A*) and HDC-KO (*B*) mice (bar = 500 μm). Note that HDC-KO mice exhibited marked gastric mucosal hyperplasia, as well as increased Cg A-positive endocrine cell counts compared with WT mice.

histamine antibodies, because HDC-KO mice lack both the HDC protein and histamine. In the present study, numerous Cg A-positive endocrine cells could be detected in the oxyntic mucosa of both WT and HDC-KO mice. In gastric mucosa, Cg A and its secretory peptide, pancreastatin, are known to be stored in the secretory vesicles of all endocrine cells, such as ECL, somatostatin-containing D, and ghrelin-containing A-like cells, among others (15, 42). Percentage of endocrine cells for the above cell types in the gastric oxyntic mucosa was ~60, 20, and 20%, respectively (11). To distinguish ECL cells from Cg A-positive cells, we attempted immunostaining of somatostatin-positive D cells and found that gastric oxyntic mucosal D cell density was similar for HDC-KO and WT mice. Similarly, it has been reported that hypergastrinemia, induced by a 10-wk omeprazole treatment, resulted in increases in oxyntic mucosa HDC mRNA levels without increases in ghrelin mRNA or somatostatin mRNA levels (20). It was also demonstrated that CCK_2R deficiency in mice did not affect the number or ultrastructure of either A-like or D cells in the oxyntic mucosa (11, 12). In addition, Cg A-gene expression was found to be regulated by serum gastrin levels in ECL cells (9, 17, 51, 54), and selective activation of Cg A-gene expression was observed in the corpus mucosa in response to gastrin (17). In consideration of such reports and the present study, it

Fig. 5. Histological comparison of the gastric mucosa of 6-mo-old WT (*A*, *C*, *E*, and *G*) and HDC-KO (*B*, *D*, *F*, and *H*) mice. hematoxylin and eosin-stained paraffin sections of gastric tissue are as shown (*A* and *B*). Immunohistochemical staining of both endocrine cells with antibody to Cg A (*C* and *D*) and parietal cells with antibody to H^+-K^+-ATPase (*E* and *F*, *G*, and *H*) was also performed (*A*–*F*, bar = 100 μm; and, *G* and *H*, bar = 10 μm). Note that the parietal and endocrine cell counts are markedly increased in the gastric mucosa of HDC-KO mice compared with WT mice. In addition, the size of H^+-K^+-ATPase-positive parietal cells in HDC-KO mice was clearly smaller than that observed for WT mice.

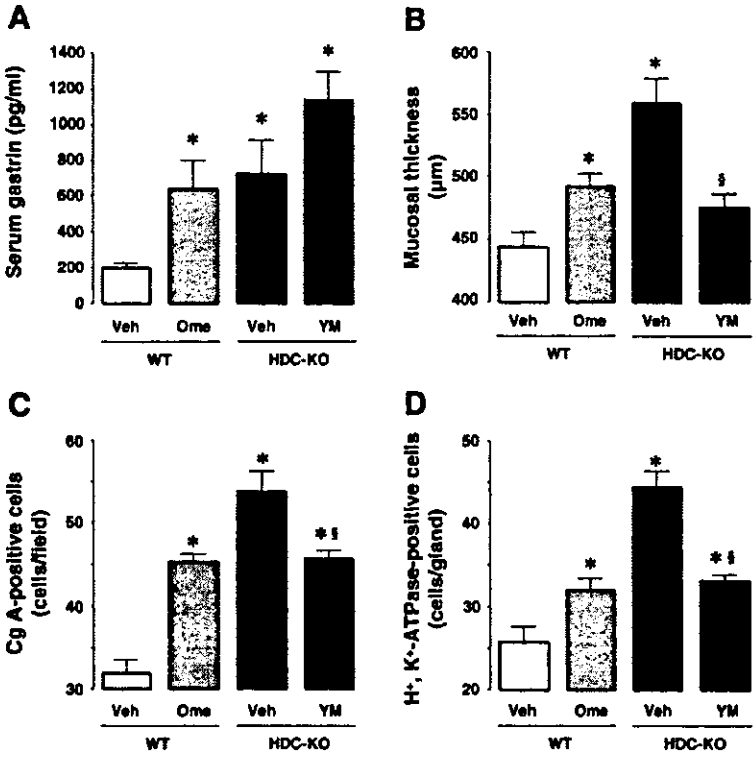

Fig. 7. Effects of omeprazole (Ome; 30 mg/kg), YM022 (YM; 30 mg/kg), and vehicle (Veh; 0.5% hydroxypropylcellurose) treatment on gastric mucosal development in WT and HDC-KO mice. Drugs were administered for 2 mo to 1-mo-old mice. Subsequently, serum gastrin levels (*A*), gastric mucosal thickness (*B*), and Cg A-positive endocrine (*C*) and parietal cell counts (*D*) were determined. Values are means ± SE. n = 6–13. Significant differences from vehicle-treated *WT and §HDC mice ($P < 0.05$).

remains most likely that the increase in Cg A-positive cells in HDC-KO mice predominantly resulted from an increase in ECL cells. However, these cells did not possess the characteristic features of ECL cells, i.e., HDC or histamine. Interestingly, using immunohistochemical and electron microscopic analysis, Chen et al. (11, 12) described in CCK_2R-KO mice, ECL-like cells that possess all of the characteristic features of ECL cells except the ability to produce histamine. Because HDC expression in ECL cells is under tight control by serum gastrin levels (4, 11, 12, 30, 31), it is reasonable that CCK_2R deficiency results in an inability to produce histamine in ECL cells. Consequently, it is possible that the ECL-like cells Chen et al. (11, 12) described represent CCK_2R-KO ECL cells, which appear to resemble the HDC-KO ECL cells in this study.

Elevation of intragastric pH, resulting from gastric acid suppression by anti-secretory drugs, such as proton pump inhibitors (34–36) or H_2R antagonists (31, 38, 39), induces hypergastrinemia (34–36) as well as ECL and parietal cell hyperplasia. In the present study, HDC deficiency resulted in intragastric pH elevation, which led to a prolonged hypergastrinemic state, which lasted up to 9 mo after birth. Accordingly, to examine whether hypergastrinemia contributes to gastric hyperplastic changes in HDC mice, we compared the differences in gastric hyperplasia for omeprazole-treated WT and HDC-KO mice. Although serum gastrin levels were similar in both groups, ECL and parietal cell counts, as well as mucosal thickness, were much higher in HDC-KO mice compared with omeprazole-treated WT mice. In addition, ECL and parietal cell hyperplasia induced in HDC-KO mice was partially suppressed by YM022 treatment. These findings are partially consistent with the reports that gastric mucosal hyperplasia induced by proton-pump inhibitors was prevented by selective CCK_2R antagonists (8, 14, 22). Because gastrin is known to stimulate gastrointestinal mucosal growth (19, 53), it appears reasonable that ECL and parietal cell hyperplasia in HDC-KO mice results from hypergastrinemia. However, in gastrin-deficient mice, no difference in total oxyntic mucosal ECL cell counts immunostained by anti-Cg A or anti-vesicular monoamine transporter 2 (VMAT2) antibodies was observed compared with the WT mice (23). Similarly, in hypergastrinemic CCK_2R-KO mice, total pancreastatin- and VMAT2-positive ECL cell counts were unchanged compared with the WT mice (11, 12). These reports suggest that factor(s) other than gastrin might directly or indirectly participate in the development of ECL cell hyperplasia in HDC-KO mice. Further studies are needed to determine the true role played by gastrin for gastric ECL cell hyperplasia induced in hypergastrinemia.

In conclusion, the present study demonstrated with HDC-KO and *W/W*^{v} mice that ECL cell-derived histamine, as opposed to mast cell-derived histamine, plays a role in gastric mucosal morphology regulation. The HDC-KO mice model provides important information for better characterization of the complicated regulation of gastric morphological homeostasis.

ACKNOWLEDGMENTS

We thank Y. Nakamura, K. Mizukoshi, and A. Ogino for technical assistance and S. Tonai and T. Ogawa for valuable suggestions. We also thank C. J.

Hurt (John Hopkins University School of Medicine, Baltimore, MD) for a critical reading of the manuscript.

REFERENCES

1. **Aihara T, Nakamura E, Amagase K, Tomita K, Fujishita T, Furutani K, and Okabe S.** Pharmacological control of gastric acid secretion for the treatment of acid-related peptic disease: past, present, and future. *Pharmacol Ther* 98: 109–127, 2003.
2. **Andersson K, Chen D, Hakanson R, Mattsson H, and Sundler F.** Enterochromaffin-like cells in the rat stomach: effect of α-fluoromethylhistidine-evoked histamine depletion. A chemical, histochemical and electron-microscopic study. *Cell Tissue Res* 270: 7–13, 1992.
4. **Andersson K, Lindstrom E, Chen D, Monstein HJ, Boketoft A, and Hakanson R.** Depletion of enterochromaffin-like cell histamine increases histidine decarboxylase and chromogranin A mRNA levels in rat stomach by a gastrin-independent mechanism. *Scand J Gastroenterol* 31: 959–965, 1996.
5. **Andersson K, Zhao CM, Chen D, Sundler F, and Hakanson R.** Effect of α-fluoromethylhistidine-evoked histamine depletion on ultrastructure of endocrine cells in acid-producing mucosa of stomach in mouse, rat and hamster. *Cell Tissue Res* 286: 375–384, 1996.
3. **Andersson K, Chen D, Mattsson H, Sundler F, and Hakanson R.** Physiological significance of ECL-cell histamine. *Yale J Biol Med* 71: 183–193, 1998.
6. **Barber BJ and Stanhope VL.** Bromcresol green assay is nonspecific for rat plasma albumin. *Am J Physiol Heart Circ Physiol* 262: H299–H302, 1992.
7. **Berenson MM, Sannella J, and Freston JW.** Menetrier's disease. Serial morphological, secretory, and serological observations. *Gastroenterology* 70: 257–263, 1976.
8. **Bjorkqvist M, Norlen P, Kitano M, Chen D, Zhao CM, de la Cour CD, Gagnemo-Persson C, and Hakanson R.** Effects of CCK2 receptor blockade on growth parameters in gastrointestinal tract and pancreas in rats. *Pharmacol Toxicol* 89: 208–213, 2001.
9. **Borch K, Stridsberg M, Burman P, and Rehfeld JF.** Basal chromogranin A and gastrin concentrations in circulation correlate to endocrine cell proliferation in type-A gastritis. *Scand J Gastroenterol* 32: 198–202, 1997.
10. **Chen D, Zhao CM, Andersson K, Sundler F, and Hakanson R.** Ultrastructure of enterochromaffin-like cells in rat stomach: effects of α-fluoromethylhistidine-evoked histamine depletion and hypergastrinemia. *Cell Tissue Res* 283: 469–478, 1996.
11. **Chen D, Zhao CM, Al-Haider W, Hakanson R, Rehfeld JF, and Kopin AS.** Differentiation of gastric ECL cells is altered in CCK_2 receptor-deficient mice. *Gastroenterology* 123: 577–585, 2002.
12. **Chen D, Zhao CM, Hakanson R, and Rehfeld JF.** Gastric phenotypic abnormality in cholecystokinin 2 receptor null mice. *Pharmacol Toxicol* 91: 375–381, 2002.
13. **Chen D, Zhao CM, Lindstrom E, and Hakanson R.** Rat stomach ECL cells up-date of biology and physiology. *Gen Pharmacol* 32: 413–422, 1999.
14. **Chen D, Zhao CM, Norlen P, Bjorkqvist M, Ding XQ, Kitano M, and Hakanson R.** Effect of cholecystokinin-2 receptor blockade on rat stomach ECL cells. A histochemical, electron-microscopic and chemical study. *Cell Tissue Res* 299: 81–95, 2000.
15. **Chen D, Zhao CM, Nylander AG, and Hakanson R.** Time course of hypertrophic and ultrastructural responses of rat stomach enterochromaffin-like cells to sustained hypergastrinemia. *Cell Tissue Res* 284: 55–63, 1996.
16. **Chen G, Kashiwagi H, Omura N, and Aoki T.** Effect of a histamine H_1 receptor antagonist on gastric endocrine cell proliferation induced by chronic acid suppression in rats. *J Gastroenterol* 35: 742–747, 2000.
17. **Dimaline R, Evans D, Forster ER, Sandvik AK, and Dockray GJ.** Control of gastric corpus chromogranin A messenger RNA abundance in the rat. *Am J Physiol Gastrointest Liver Physiol* 264: G583–G588, 1993.
18. **Dockray GJ.** Topical Review: gastrin and gastric epithelial physiology. *J Physiol* 518: 315–324, 1999.
19. **Dockray GJ, Varro A, Dimaline R, and Wang T.** The gastrins: their production and biological activities. *Annu Rev Physiol* 63: 119–139, 2001.
20. **Dornonville de la Cour C, Bjorkqvist M, Sandvik AK, Bakke I, Zhao CM, Chen D, and Hakanson R.** A-like cells in the rat stomach contain ghrelin and do not operate under gastrin control. *Regul Pept* 99: 141–150, 2001.
21. **Doumas BT, Watson WA, and Biggs HG.** Albumin standards and the measurement of serum albumin with bromcresol green. *Clin Chim Acta* 31: 87–96, 1971.
22. **Eissele R, Patberg H, Koop H, Krack W, Lorenz W, McKnight AT, and Arnold R.** Effect of gastrin receptor blockade on endocrine cells in rats during achlorhydria. *Gastroenterology* 103: 1596–1601, 1992.
23. **Friis-Hansen L, Sundler F, Li Y, Gillespie PJ, Saunders TL, Greenson JK, Owyang C, Rehfeld JF, and Samuelson LC.** Impaired gastric acid secretion in gastrin-deficient mice. *Am J Physiol Gastrointest Liver Physiol* 274: G561–G568, 1998.
24. **Furutani K, Aihara T, Nakamura E, Tanaka S, Ichikawa A, Ohtsu H, and Okabe S.** Crucial role of histamine for regulation of gastric acid secretion ascertained by histidine decarboxylase-knockout mice. *J Pharmacol Exp Ther* 307: 331–338, 2003.
25. **Hakanson R, Bottcher G, Ekblad E, Panula P, Simonsson M, Dohlsten M, Hallberg T, and Sundler F.** Histamine in endocrine cells in the stomach. A survey of several species using a panel of histamine antibodies. *Histochemistry* 86: 5–17, 1986.
26. **Hinkle KL, Bane GC, Jazayeri A, and Samuelson LC.** Enhanced calcium signaling and acid secretion in parietal cells isolated from gastrin-deficient mice. *Am J Physiol Gastrointest Liver Physiol* 284: G145–G153, 2003.
27. **Hunyady B, Zolyomi A, Czimmer J, Mozsik G, Kozicz T, Buzas E, Tanaka S, Ichikawa A, Nagy A, Palkovits M, and Falus A.** Expanded parietal cell pool in transgenic mice unable to synthesize histamine. *Scand J Gastroenterol* 38: 133–140, 2003.
28. **Karam SM and Leblond CP.** Identifying and counting epithelial cell types in the "corpus" of the mouse stomach. *Anat Rec* 232: 231–246, 1992.
29. **Kobayashi T, Tonai S, Ishihara Y, Koga R, Okabe S, and Watanabe T.** Abnormal functional and morphological regulation of the gastric mucosa in histamine H2 receptor-deficient mice. *J Clin Invest* 105: 1741–1749, 2000.
30. **Kolby L, Wangberg B, Ahlman H, Modlin IM, Granerus G, Theodorsson E, and Nilsson O.** Histidine decarboxylase expression and histamine metabolism in gastric oxyntic mucosa during hypergastrinemia and carcinoid tumor formation. *Endocrinology* 137: 4435–4442, 1996.
31. **Kolby L, Wangberg B, Ahlman H, Modlin IM, Theodorsson E, and Nilsson O.** Altered influence of CCK-B/gastrin receptors on HDC expression in ECL cells after neoplastic transformation. *Regul Pept* 85: 115–123, 1999.
32. **Ladas SD, Tassios PS, Malamou HC, Protopapa DP, and Raptis SA.** Omeprazole induces a long-term clinical remission of protein-losing gastropathy of Menetrier's disease. *Eur J Gastroenterol Hepatol* 9: 811–813, 1997.
33. **Larsen B, Tarp U, and Kristensen E.** Familial giant hypertrophic gastritis (Menetrier's disease). *Gut* 28: 1517–1521, 1987.
34. **Larsson H, Carlsson E, Hakanson R, Mattsson H, Nilsson G, Seensalu R, Wallmark B, and Sundler F.** Time-course of development and reversal of gastric endocrine cell hyperplasia after inhibition of acid secretion. Studies with omeprazole and ranitidine in intact and antrectomized rats. *Gastroenterology* 95: 1477–1486, 1988.
35. **Larsson H, Carlsson E, Mattsson H, Lundell L, Sundler F, Sundell G, Wallmark B, Watanabe T, and Hakanson R.** Plasma gastrin and gastric enterochromaffinlike cell activation and proliferation. Studies with omeprazole and ranitidine in intact and antrectomized rats. *Gastroenterology* 90: 391–399, 1986.
36. **Larsson H, Hakanson R, Mattsson H, Ryberg B, Sundler F, and Carlsson E.** Omeprazole: its influence on gastric acid secretion, gastrin and ECL cells. *Toxicol Pathol* 16: 267–272, 1988.
37. **Lindstrom E, Andersson K, Chen D, Monstein HJ, Boketoft A, and Hakanson R.** α-Fluoromethylhistidine elevates histidine decarboxylase mRNA and chromogranin A mRNA levels in rat oxyntic mucosa. *Inflamm Res* 46, *Suppl* 1: S107–S108, 1997.
38. **Modlin IM, Kumar RR, Soroka CJ, Ahlman H, Nilsson O, and Goldenring JR.** Histamine as an intermediate growth factor in genesis of gastric ECLomas associated with hypergastrinemia in mastomys. *Dig Dis Sci* 39: 1446–1453, 1994.
39. **Modlin IM, Zhu Z, Tang LH, Kidd M, Lawton GP, Miu K, Powers RE, Goldenring JR, Pasikhov D, and Soroka CJ.** Evidence for a regulatory role for histamine in gastric enterochromaffin-like cell proliferation induced by hypergastrinemia. *Digestion* 57: 310–321, 1996.
40. **Morini G, Grandi D, and Schunack W.** Ligands for histamine H_3 receptors modulate cell proliferation and migration in rat oxyntic mucosa. *Br J Pharmacol* 137: 237–244, 2002.

41. **Nishida A, Kobayashi-Uchida A, Akuzawa S, Takinami Y, Shishido T, Kamato T, Ito H, Yamano M, Yuki H, Nagakura Y, Honda K, and Miyata K.** Gastrin receptor antagonist YM022 prevents hypersecretion after long-term acid suppression. *Am J Physiol Gastrointest Liver Physiol* 264: G699–G705, 1995.
42. **Norlen P, Curry WJ, Chen D, Zhao CM, Johnston CF, and Hakanson R.** Expression of the chromogranin A-derived peptides pancreastatin and WE14 in rat stomach ECL cells. *Regul Pept* 70: 121–133, 1997.
43. **Norlen P, Lindstrom E, Zhao C, Kitano M, Chen D, Andersson K, and Hakanson R.** α-Fluoromethylhistidine depletes histamine from secreting but not from non-secreting rat stomach ECL cells. *Eur J Pharmacol* 400: 1–10, 2000.
44. **Ogawa T, Maeda K, Tonai S, Kobayashi T, Watanabe T, and Okabe S.** Utilization of knockout mice to examine the potential role of gastric histamine H_2-receptors in Menetrier's disease. *J Pharm Sci* 91: 61–70, 2003.
45. **Ohtsu H, Tanaka S, Terui T, Hori Y, Makabe-Kobayashi Y, Pejler G, Tchougounova E, Hellman L, Gertsenstein M, Hirasawa N, Sakurai E, Buzas E, Kovacs P, Csaba G, Kittel A, Okada M, Hara M, Mar L, Numayama-Tsuruta K, Ishigaki-Suzuki S, Ohuchi K, Ichikawa A, Falus A, Watanabe T, and Nagy A.** Mice lacking histidine decarboxylase exhibit abnormal mast cells. *FEBS Lett* 502: 53–56, 2001.
46. **Prinz C, Zanner R, and Gratzl M.** Physiology of gastric enterochromaffin-like cells. *Annu Rev Physiol* 65: 371–382, 2003.
47. **Sachs G, Prinz C, Loo D, Bamberg K, Besancon M, and Shin JM.** Gastric acid secretion: activation and inhibition. *Yale J Biol Med* 67: 81–95, 1994.
48. **Scott HW Jr, Shull HJ, Law DH IV, Burko H and Page DL.** Surgical management of Menetrier's disease with protein-losing gastropathy. *Ann Surg* 181: 765–767, 1975.
49. **Shimada M, Kitamura Y, Yokoyama M, Miyano Y, Maeyama K, Yamatodani A, Takahashi Y, and Tatsuta M.** Spontaneous stomach ulcer in genetically mast-cell depleted *W/W*^{v} mice. *Nature* 283: 662–664, 1980.
50. **Stechschulte DJ Jr, Morris DC, Jilka RL, Stechschulte DJ, and Dileepan KN.** Impaired gastric acid secretion in mast cell-deficient mice. *Am J Physiol Gastrointest Liver Physiol* 259: G41–G47, 1990.
51. **Syversen U, Mignon M, Bonfils S, Kristensen A, and Waldum HL.** Chromogranin A and pancreastatin-like immunoreactivity in serum of gastrinoma patients. *Acta Oncol* 32: 161–165, 1993.
52. **Tanaka S, Hamada K, Yamada N, Sugita Y, Tonai S, Hunyady B, Palkovits M, Falus A, Watanabe T, Okabe S, Ohtsu H, Ichikawa A, and Nagy A.** Gastric acid secretion in L-histidine decarboxylase-deficient mice. *Gastroenterology* 122: 145–155, 2002.
53. **Watkinson A and Dockray GJ.** Functional control of chromogranin A and B concentrations in the body of the rat stomach. *Regul Pept* 40: 51–61, 1992.
54. **Wang TC and Brand SJ.** Function and regulation of gastrin in transgenic mice: a review. *Yale J Biol Med* 65: 705–713, 1992.
55. **Wolfsen HC, Carpenter HA, and Talley NJ.** Menetrier's disease: a form of hypertrophic gastropathy or gastritis? *Gastroenterology* 104: 1310–1319, 1993.

nature medicine

Free fatty acids regulate gut incretin glucagon-like peptide-1 secretion through GPR120

Akira Hirasawa[1,2,3], Keiko Tsumaya[1], Takeo Awaji[4], Susumu Katsuma[5], Tetsuya Adachi[5], Masateru Yamada[1], Yukihiko Sugimoto[6], Shunichi Miyazaki[4] & Gozoh Tsujimoto[2,3]

Reprinted from *Nature Medicine*, Volume 11, January 2005

nature medicine

Free fatty acids regulate gut incretin glucagon-like peptide-1 secretion through GPR120

Akira Hirasawa[1,2,3], Keiko Tsumaya[1], Takeo Awaji[4], Susumu Katsuma[5], Tetsuya Adachi[5], Masateru Yamada[1], Yukihiko Sugimoto[6], Shunichi Miyazaki[4] & Gozoh Tsujimoto[2,3]

Diabetes, a disease in which the body does not produce or use insulin properly, is a serious global health problem[1–3]. Gut polypeptides secreted in response to food intake, such as glucagon-like peptide-1 (GLP-1), are potent incretin hormones that enhance the glucose-dependent secretion of insulin from pancreatic beta cells[4–6]. Free fatty acids (FFAs) provide an important energy source and also act as signaling molecules in various cellular processes, including the secretion of gut incretin peptides[7,8]. Here we show that a G-protein-coupled receptor, GPR120, which is abundantly expressed in intestine, functions as a receptor for unsaturated long-chain FFAs. Furthermore, we show that the stimulation of GPR120 by FFAs promotes the secretion of GLP-1 *in vitro* and *in vivo*, and increases circulating insulin. Because GLP-1 is the most potent insulinotropic incretin[9,10], our results indicate that GPR120-mediated GLP-1 secretion induced by dietary FFAs is important in the treatment of diabetes.

GPR120 is an orphan G-protein-coupled receptor[11], which we isolated from a human genomic DNA fragment. We isolated cDNAs from human and mouse. Analyses for the tissue distribution of *Gpr120* mRNA by real-time polymerase chain reaction with reverse transcription (RT-PCR) showed an abundant expression of *Gpr120* mRNA in the intestinal tract in mouse (**Fig. 1a**) and human (**Fig. 1b**). *Gpr120* mRNA was also found to be abundantly expressed in the mouse intestinal endocrine cell line STC-1, but was not detected in other cell lines, including NCI-H716, CaCo-2, HT29, IEC-6, IEC-18, Intestine 407 or the pancreatic beta-cell line MIN6 (data not shown).

To identify endogenous ligands for Gpr120, we added over 1,000 chemical compounds to HEK 293 cells stably expressing Gpr120–enhanced green fluorescent protein (EGFP) and examined changes in the amount of the internalized fluorescently labeled receptor in the endocytic compartment with a quantitative cytometric technique (ArrayScan II system)[12,13]. As a result, long-chain FFAs were found to evoke specific internalization of the Gpr120-EGFP conjugate, and this FFA-mediated internalization was blocked by a 1% concentration of bovine serum albumin (BSA), which binds FFAs effectively (**Fig. 1c**). Using HEK 293 cells stably expressing the mouse Gpr120-Gα16 fusion protein[14], we further examined the effects of chemical compounds on the concentration of intracellular Ca^{2+} ($[Ca^{2+}]_i$) response by using a fluorometric imaging plate reader system. In agreement with the receptor internalization analysis, long-chain FFAs were found to evoke a specific rise in $[Ca^{2+}]_i$ in a dose-dependent fashion (**Fig. 1d,e**). Apparent stimulatory activities were detected for saturated FFAs with a chain length of C_{14} to C_{18}, and for unsaturated FFAs of C_{16} to C_{22} (**Supplementary Table 1** online). The $[Ca^{2+}]_i$ response evoked by long-chain FFAs was inhibited by BSA at concentrations higher than 0.1% (**Fig. 1f**).

We could not detect either a stimulatory or an inhibitory effect of long-chain FFAs on cAMP production in HEK 293 cells transiently expressing mouse and human *Gpr120* cDNAs (data not shown). But the long-chain FFAs palmitoleic acid, α-linolenic acid and docosahexaenoic acid increased the amount of phosphorylated extracellular signal-regulated kinase (ERK) (p44/42) in HEK 293 cells transiently expressing mouse Gpr120 (**Fig. 1g**). By contrast, linolenic acid methyl ester did not show stimulatory activity, suggesting that the carboxyl group is indispensable for this function. Together, these results show that Gpr120 functions as a specific receptor for long-chain FFAs.

FFAs stimulate the release of incretin peptide hormones such as cholecystokinin and GLP-1 from the gastrointestinal tract[15–17]. STC-1, the mouse enteroendocrine cell line of intestinal origin, has been used as a model of this process[18]. Because secretion of gut peptide hormones from STC-1 cells was shown to be evoked through the triggering of an FFA-specific Ca^{2+} signal transduction pathway that may involve a putative receptor[18], we examined whether the secretion of GLP-1 from STC-1 cells is mediated through the Gpr120 receptor. Neither medium-chain nor saturated long-chain FFAs had much effect on the secretion of GLP-1 from STC-1 cells, whereas unsaturated long-chain FFAs showed a dose-dependent stimulatory effect, with α-linolenic acid having the most potency (**Fig. 2a**). Furthermore, the FFAs that were shown to have a stimulatory effect on $[Ca^{2+}]_i$ response and on ERK activa-

[1]Department of Molecular, Cell Pharmacology, National Research Institute for Child Health and Development, 3-35-31, Taishi-do, Setagaya-ku, Tokyo 154-8567, Japan. [2]Department of Genomic Drug Discovery Science, Graduate School of Pharmaceutical Sciences, Kyoto University, 46-29 Yoshida Shimoadachi-cho, Sakyo-ku, Kyoto 606-8501, Japan. [3]Shinanomachi Research Park 7S7, Keio University, 35 Shinanomachi, Shinjuku-ku, Tokyo 160-8582, Japan. [4]Department of Physiology, Tokyo Women's Medical University School of Medicine, 8-1 Kawada-cho, Shinjuku-ku, Tokyo 162-8666, Japan. [5]Bioinformatics Center, Institute for Chemical Research, Kyoto University, Uji, Kyoto 611-0011, Japan. [6]Department of Physiological Chemistry, Graduate School of Pharmaceutical Sciences, Kyoto University, 46-29 Yoshida Shimoadachi-cho, Sakyo-ku, Kyoto 606-8501, Japan. Correspondence should be addressed to G.T. (gtsuji@pharm.kyoto-u.ac.jp).

Published online 26 December 2004; doi:10.1038/nm1168

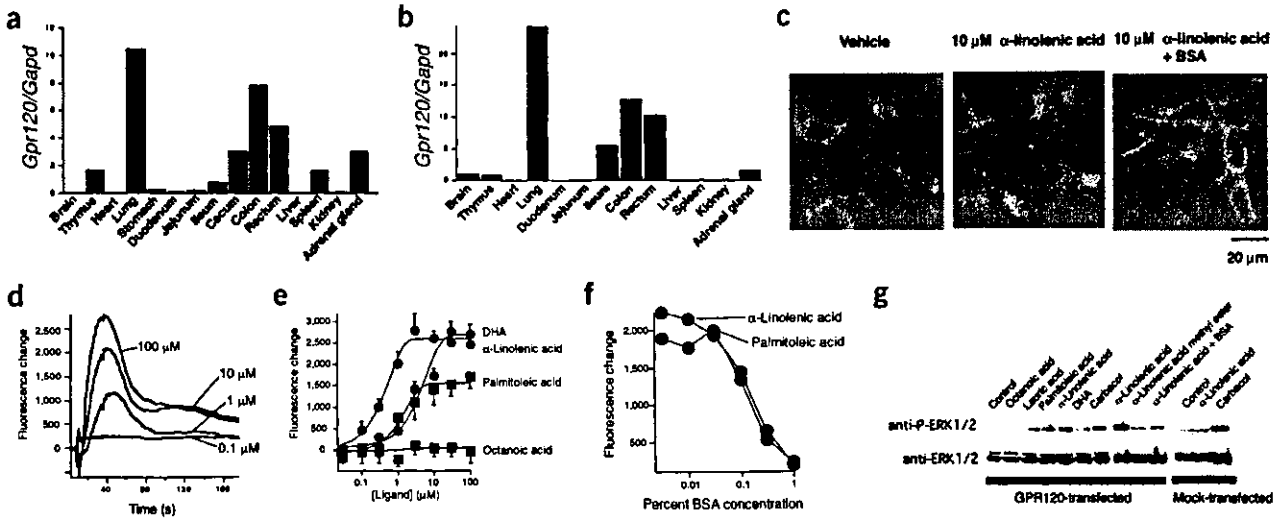

Figure 1 Tissue distribution and signal transduction of *Gpr120*. (**a**,**b**) Real-time RT-PCR of *Gpr120* mRNA in mouse (**a**) and human (**b**) tissues. (**c**) α-Linolenic acid induces internalization of EGFP-tagged Gpr120. Gpr120-EGFP-expressing HEK 293 cells treated with vehicle (dimethyl sulfoxide; left), treated with 10 μM α-linolenic acid in the absence (middle) or presence (right) of 0.1% BSA. (**d**) $[Ca^{2+}]_i$ response induced by α-linolenic acid in HEK 293 cells expressing Gpr120-Gα16. (**e**) FFA-induced $[Ca^{2+}]_i$ response is concentration dependent. DHA, docosahexaenoic acid. (**f**) Effects of BSA on α-linolenic acid– and palmitoleic acid–induced $[Ca^{2+}]_i$ rise in HEK 293 cells stably expressing Gpr120-Gα16. (**g**) Representative western blots for FFA-induced ERK activation in HEK 293 cells transiently expressing Gpr120.

tion in GPR120-expressing HEK 293 cells (**Fig. 1e,g**) potently induced GLP-1 secretion from STC-1 cells (**Fig. 2a**). The α-linolenic acid–induced secretion of GLP-1 from STC-1 cells was significantly inhibited ($P < 0.05$) either by BSA treatment or by using a Ca^{2+}-free medium; however, neither nifedipine (an L-type calcium channel blocker), thapsigargin (an endoplasmic reticulum Ca^{2+} ATPase inhibitor), PD098059 (an ERK kinase inhibitor) nor U-73122 (a phospholipase C inhibitor) had inhibitory effect (**Fig. 2b**). The activation of ERK by FFAs in STC-1 cells showed an order of potency similar to that observed in HEK 293 cells transiently transfected with mouse Gpr120 (**Fig. 2c**). All of the unsaturated long-chain FFAs examined increased the phosphorylation of ERK in STC-1 cells, with α-linolenic acid again having the most potent stimulatory effect.

Gpr120 mRNA was abundantly expressed in STC-1 cells, but was not detectable in the pancreatic beta cell line MIN6 (**Fig. 2d**). MIN6 cells express the receptor Gpr40 abundantly (**Fig. 2d**), whose ligands were also shown to be FFAs[19]. As we found STC-1 cells express both Gpr120 and Gpr40 G-protein-coupled receptors for FFAs (**Fig. 2d**), we assessed the effects of inhibiting the expression and the function of either Gpr120 or Gpr40 in STC-1 cells by using small interfering RNAs (siRNAs). We first examined the inhibitory effect of these siRNAs on the FFA-related Ca^{2+} signal pathway in STC-1 cells, as an increase in $[Ca^{2+}]_i$ has an important role in triggering hormone secretion from STC-1 cells. STC-1 cells showed a spontaneous oscillation in $[Ca^{2+}]_i$, and the application of α-linolenic acid provoked a rapid rise in $[Ca^{2+}]_i$ (**Fig. 3a**). Next, we transfected STC-1 cells with either of the siRNA vectors together with a yellow fluorescent protein expression vector, and then individual cells expressing yellow fluorescent protein were examined by microscopic $[Ca^{2+}]_i$ imaging analysis. The increase in $[Ca^{2+}]_i$ in STC-1 cells induced by α-linolenic acid was eliminated by siRNA specific for mouse Gpr120, but not by an siRNA specific for mouse Gpr40 (**Fig. 3b–d**). In all cells examined, the bombesin-induced $[Ca^{2+}]_i$ response was unaffected. We next examined the inhibitory effect of these siRNAs on FFA-stimulated GLP-1 secretion in STC-1 cells. Real-time RT-PCR of the STC-1 cells showed that transfection with Gpr120-specific siRNA reduced *Gpr120* mRNA expression by about 20% with little effect on *Gpr40* mRNA expression; on the other hand, Gpr40-specific siRNA reduced *Gpr40* mRNA expression by about 20% with little effect on *Gpr120* mRNA expression (**Fig. 3e**). Corresponding with the reduction of mRNA expression, transfection with Gpr120-specific siRNA significantly reduced ($P < 0.05$) α-linolenic acid-induced GLP-1 secretion from STC-1 cell (**Fig. 3e**). On the other hand, Gpr40-specific siRNA did not show any inhibitory effect (**Fig. 3e**). These results indicate that the FFA-induced $[Ca^{2+}]_i$ increase and GLP-1 secretion in STC-1 cells is mediated through Gpr120. Furthermore, to examine the link between Gpr120 and FFA-induced GLP-1 secretion in endocrine cells, we performed experiments using another cell line of NCI-H716, a human intestinal cell line that expresses the gene encoding proglucagon and secretes GLP-1 in a regulated manner[20]. NCI-H716 cells have little expression of *Gpr40* and *Gpr120* mRNA detected by RT-PCR assay, and the cells did not respond to lower concentrations of FFA (<1 mM)[21]. Transfection with GPR120, but not GPR40, conferred NCI-H716 cells with the ability to secrete GLP-1 in response to α-linolenic acid (**Fig. 3f**).

We examined the effect of FFAs on gut peptide secretion *in vivo*. We first assessed whether GPR120 and GLP-1 are colocalized in colon by double staining experiments coupling *in situ* hybridization for *GPR120* mRNA with immunohistochemistry for GLP-1. The sequential *in situ* hybridization–immunohistochemistry study showed double colocalized stainings for *GPR120* mRNA (**Fig. 4a**) and GLP-1 (**Fig. 4a**) in human colonic intraepithelial neuroendocrine cells. On the other hand, positive signals for *GPR40* by *in situ* hybridization were not observed in the colonic specimen (data not shown). This coexpression of *GPR120* mRNA and GLP-1 was further confirmed by RT-PCR of GLP-1-positive stained areas collected by laser capture microdissection[22]. The real-time RT-PCR assay showed markedly abundant expression of *GPR120* in the GLP-1-positive cells in human colon, whereas it was present only at a detectable level in the GLP-1-negative cells (**Fig. 4b**). Furthermore, we examined the *in vivo* effect of FFAs on GLP-1 release in C57/B6 mice.

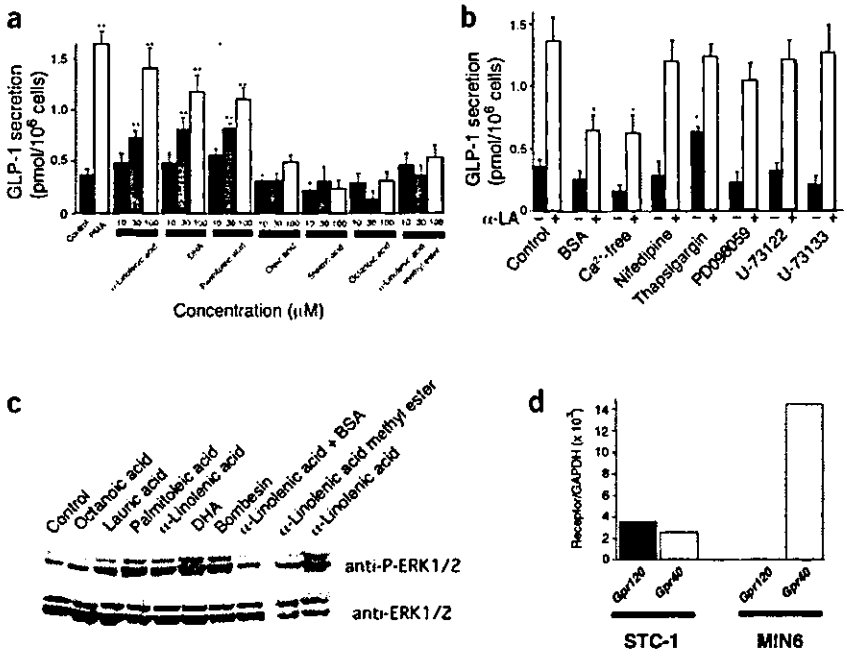

Figure 2 Long FFA-induced GLP-1 secretion and ERK activation in STC-1 cells. (**a**) FFA-induced GLP-1 secretion from STC-1 cells. DHA, docosahexaenoic acid. (**b**) Effects of BSA, extracellular Ca^{2+} and inhibitors on FFA-induced GLP-1 secretion from STC-1 cells. We performed preincubation in Hank balanced salt solution without Ca^{2+} or containing 0.1% BSA, 50 μM PD098059, 10 μM nifedipine, 1 μM thapsigargin, 10 μM U-73122, 10 μM U-73133 (inactive control for U-73122). $*P < 0.05$. $**P < 0.01$. Error bars represent s.e.m. (**c**) FFA-activated ERK in STC-1 cells. (**d**) Real-time RT-PCR analysis of *Gpr120* and *Gpr40* mRNA expression in STC-1 and MIN6 cells.

We monitored the plasma concentrations of GLP-1 and insulin in portal vein and inferior vena cava after the oral administration of α-linolenic acid. The plasma concentrations of GLP-1 in both veins had significantly increased ($P < 0.05$; Fig. 4c). Also, the plasma concentrations of insulin had significantly increased ($P < 0.01$; Fig. 4d). In contrast to α-linolenic acid, the oral administration of stearic acid and octanoic acid was less effective at inducing GLP-1 secretion *in vivo* (Fig. 4e), a finding in keeping with the results of the *in vitro* experiments. Our data indicate that GPR120 functions as a specific receptor for long-chain FFAs and can potently regulate the secretion of incretin hormone GLP-1 from the gastrointestinal tract.

Recently, G-protein-coupled receptors of the GPR40-43 family have been shown to be activated by FFAs[19,23–25]. As GPR120 and GPR40 are activated by similar properties of FFAs, and GPR40 directly[19] and GPR120 indirectly promote glucose-stimulated insulin secretion; both GPR120 and GPR40 will be important for assessing the mechanism of FFA-mediated insulin secretion and for the treatment of diabetes. Moreover, given the significance of GLP-1 in appetite and feeding control[9], GPR120 represents a promising new target for the treatment of obesity and other eating disorders, such as bulimia.

METHODS

Real-time RT-PCR. Total RNA was extracted, and reverse-transcription reactions were performed using the Superscript-II enzyme (Invitrogen). Quantitative detection of specific mRNA transcripts was carried out by real-time PCR using DNA Engine Opticon2 System and DyNAmo HS SYBR Green qPCR kit (MJ Research).

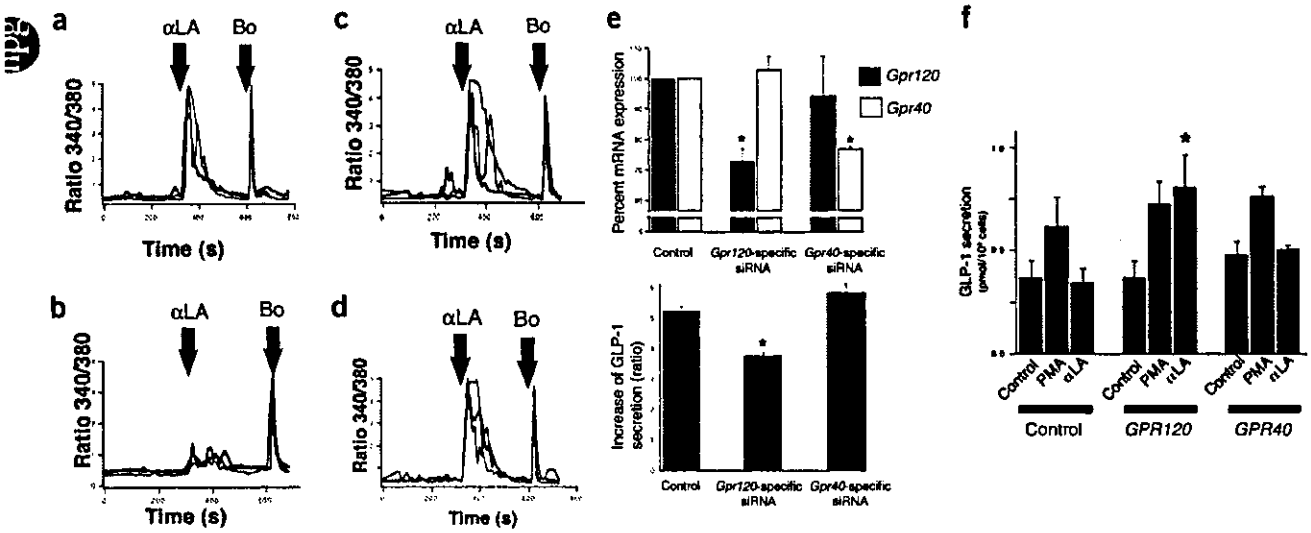

Figure 3 Gpr120, but not Gpr40, mediates FFA-induced $[Ca^{2+}]_i$ response and GLP-1 secretion. (**a–d**) Single-cell imaging of $[Ca^{2+}]_i$ response induced by 10 μM α-linolenic acid (αLA) and 1 μM bombesin (Bo) in STC-1 cells. Cells were transfected with either Gpr120-specific (**b**), Gpr40-specific (**c**) or a control (**d**) siRNA expression vector. (**e**) Effects of siRNA either on mRNA expression (upper) or on α-linolenic acid-induced GLP-1 secretion (lower) in STC-1 cells. (**f**) Effect of transfection with either *Gpr120* or *Gpr40* cDNA on the α-linolenic acid (αLA)-induced GLP-1 secretion in NCI-H716 cells. $*P < 0.05$. Error bars represent s.e.m.

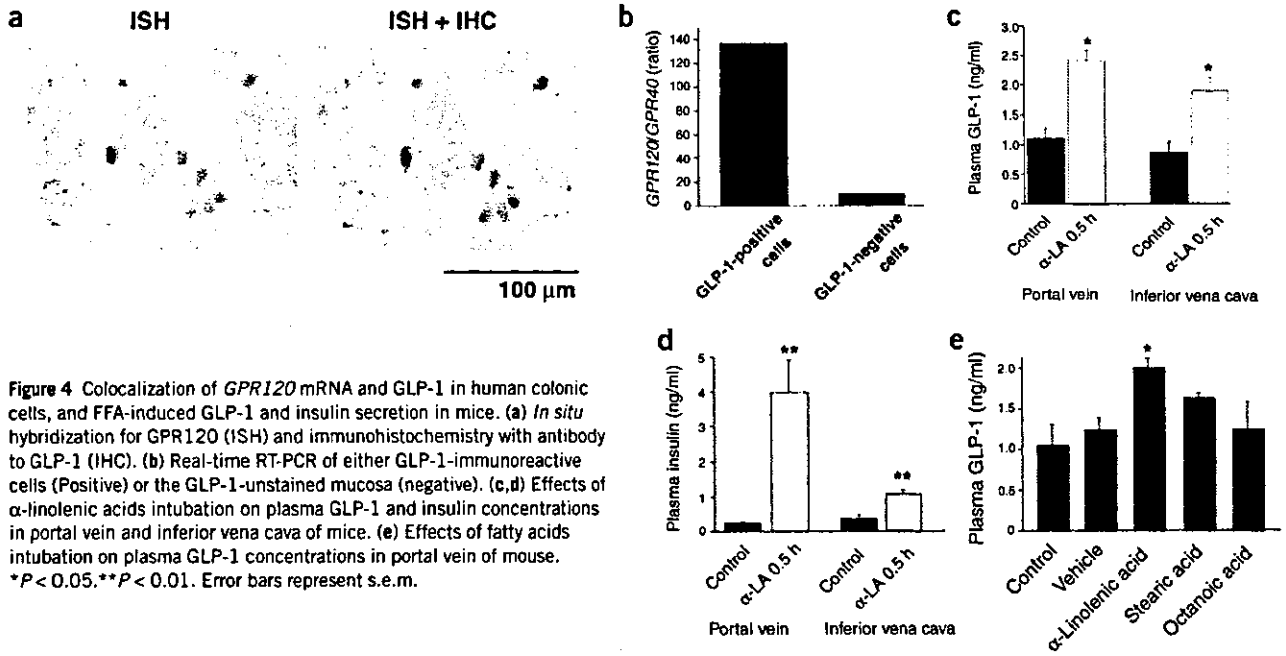

Figure 4 Colocalization of *GPR120* mRNA and GLP-1 in human colonic cells, and FFA-induced GLP-1 and insulin secretion in mice. **(a)** *In situ* hybridization for GPR120 (ISH) and immunohistochemistry with antibody to GLP-1 (IHC). **(b)** Real-time RT-PCR of either GLP-1-immunoreactive cells (Positive) or the GLP-1-unstained mucosa (negative). **(c,d)** Effects of α-linolenic acids intubation on plasma GLP-1 and insulin concentrations in portal vein and inferior vena cava of mice. **(e)** Effects of fatty acids intubation on plasma GLP-1 concentrations in portal vein of mouse. $^{*}P < 0.05$. $^{**}P < 0.01$. Error bars represent s.e.m.

Receptor localization analysis. For the receptor-EGFP expression constructs, *Gpr120* cDNAs were ligated into the pEGFP-N3 vector (BD Japan). HEK 293 cells stably or transiently expressing EGFP constructs were detected by fluorescence analysis[26,27]. For ligand screening, cells were seeded at a density of 10^4 cells/well on 96-well plates in serum-free medium 24 h before drug treatment. After 1 h incubation with drugs, we fixed the cells with 2% formaldehyde in phosphate-buffered saline and analyzed them by an ArrayScan cytometer (Cellomics)[13]. Using the ArrayScan software, we monitored changes in the amount of receptor internalization. For more detailed subcellular localization of the receptor, we used confocal microscopy FLUOVIEW/LSM (Olympus).

$[Ca^{2+}]_i$ analysis. The GPR120-Gα16 expression vector was stably transfected into HEK 293 cells and subjected to $[Ca^{2+}]_i$ analysis. Cells were seeded at a density of 10^4 cells/well on 96-well plates in serum-free medium 24 h before the fluorometric imaging plate reader (Molecular Devices) assay. Changes in $[Ca^{2+}]_i$ were also monitored by measuring fura-2 fluorescence using CAF-110 (Jasco) as described previously[28]. $[Ca^{2+}]_i$ imaging and data acquisition was carried out as described previously[29]. Data analysis was performed using US National Institutes of Health Image program and Igor Pro (WaveMetrics).

ERK activity. Activation of ERK in HEK 293 and STC-1 cells after treatment with 10 μM of each FFA was determined[30]. In brief, total cell extracts were prepared and Thr202/Tyr204 phosphorylated ERK1/2 (P-ERK1/2) proteins or total ERK1/2 proteins were detected by western blotting.

siRNA experiments. DNA oligonucleotides targeting Gpr120 and Gpr40 at different locations were synthesized and inserted into the RNA polymerase III promoter-based siRNA expression vector pSilencer1.0 (Ambion). The sequences of siRNA expression vectors pSi-GPR120C or pSi-GPR40A are

5′-GGGCGACCACCGGTTGGTGTTCAAGAGACACCAACCGGTGGTC GCCCTTTTTT-3′ and 5′-CGCCAGTTGTGACATTCTTTTCAAGAGAAAG AATGTCACAACTGGCGTTTTTT-3′ , respectively. Also, we used pSilencer Negative Control Vector as control siRNA. Transfection was performed by either Lipofectamine PLUS (Invitrogen Corporation) or DoFect GT1 (Dojindo Laboratories). Also, we confirmed that the siRNA specific for mouse Gpr40 inhibited the α-linolenic acid–enhanced glucose-induced increase in $[Ca^{2+}]_i$ in MIN6 cells (data not shown).

GLP-1 secretion. We washed STC-1 cells three times with Hank balanced salt solution, transferred them to growth medium and incubated them for 60 min at 37 °C in Hank balanced salt solution containing various concentrations of fatty acid sonicated just before use with a probe sonicator (Tomy Seiko). After incubation, conditioned medium was collected and concentration of GLP-1 was determined by enzyme immunoassay with a specific GLP-1 (7–36) amide Enzyme Immunoassay Kit (YK 160; Yanaihara Institute).

***In situ* hybridization, immunohistochemistry and laser capture microdissection.** For detecting *GPR120* and *GPR40* mRNA, digoxigenin-labeled probes were synthesized by means of a digoxigenin RNA Labeling Kit (Roche Diagnostics). We fixed human and mouse colons in 4% paraformaldehyde, and sliced paraffin sections at a thickness of 20 μm. The sections were treated with Proteinase K, hybridized with the probe and the signal was detected with NBT/BCIP solution (Roche Diagnostics). The same sections were then incubated by a rabbit GLP-1 (7–36) amide–specific antibody (Peninsula Laboratories) and GLP-1 immunoreactivity was visualized with DAB solution. We performed laser capture under direct microscopic visualization of the GLP-1-stained areas by melting selected regions onto a thermoplastic film mounted on optically transparent laser capture microdissection caps using the PixCell II LCM System (Arcturus Engineering). Total RNA was extracted and subjected to RT-PCR analysis.

GLP-1 secretion *in vivo*. Eight-week-old male C57/B6 mice (Sankyo Lab) were given 100 nmol/g fatty acids in vehicle (PEG) through a stomach tube after being deprived of food for 24 h. We took blood from the portal vein and the central vein using a heparinized syringe at 0.5 and 2 h after intubation under anesthesia with diethyl ether. Plasma was obtained by centrifugation of heparinized blood at 4 °C for 20 min at 1,200*g* and subjected to the GLP-1 enzyme immunoassay and insulin enzyme immunoassay (Morinaga). All experimentation was performed in accordance with approved institutional guidelines at the National Research Institute for Child Health and Development.

Statistics. We used one-way or two-way analysis of variance (ANOVA) to evaluate treatment effects. If the ANOVA value was significant, comparisons between the control and treatment group were performed using ANOVA followed by Dunnett's *t*-test to localize the significant difference. $P < 0.05$ was considered significant. All statistics were run with R (R project).

URLs. US National Institutes of Health Image http://rsb.info.nih.gov/nih-image/ R project http://www.r-project.org/

Accession numbers. The human and mouse *GPR120* cDNA sequences were deposited in GenBank under numbers AB115768 and AB115769, respectively.

Note: Supplementary information is available on the Nature Medicine website.

ACKNOWLEDGMENTS

We thank S. Mine, T. Tanaka, Y. Kitagawa and S. Suzuki for their technical assistance. This study was performed through Special Coordination Funds for Promoting Science and Technology from the Ministry of Education, Culture, Sports, Science and Technology, the Japanese Government (G.T.). S.K. and T.A. are supported by the 21st Century Center of Excellence Program "Knowledge Information Infrastructure for Genome Science."

COMPETING INTERESTS STATEMENT

The authors declare that they have no competing financial interests.

Received 8 September; accepted 22 November 2004
Published online at http://www.nature.com/naturemedicine/

1. Zimmet, P., Alberti, K.G. & Shaw, J. Global and societal implications of the diabetes epidemic. *Nature* **414**, 782–787 (2001).
2. Gadsby, R. Epidemiology of diabetes. *Adv. Drug. Deliv. Rev.* **54**, 1165–1172 (2002).
3. Jovanovic, L. & Gondos, B. Type 2 diabetes: the epidemic of the new millennium. *Ann. Clin. Lab. Sci.* **29**, 33–42 (1999).
4. Creutzfeldt, W. & Ebert, R. New developments in the incretin concept. *Diabetologia* **28**, 565–573 (1985).
5. Kieffer, T.J. & Habener, J.F. The glucagon-like peptides. *Endocr. Rev.* **20**, 876–913 (1999).
6. Kreymann, B., Williams, G., Ghatei, M.A. & Bloom, S.R. Glucagon-like peptide-1 7-36: a physiological incretin in man. *Lancet* **2**, 1300–1304 (1987).
7. Nunez, E.A. Biological complexity is under the 'strange attraction' of non-esterified fatty acids. *Prostaglandins. Leukot. Essent. Fatty Acids* **57**, 107–110 (1997).
8. Thomsen, C., Storm, H., Holst, J.J. & Hermansen, K. Differential effects of saturated and monounsaturated fats on postprandial lipemia and glucagon-like peptide 1 responses in patients with type 2 diabetes. *Am. J. Clin. Nutr.* **77**, 605–611 (2003).
9. MacDonald, P.E. *et al.* The multiple actions of GLP-1 on the process of glucose-stimulated insulin secretion. *Diabetes* **51** Suppl 3, S434–S442 (2002).
10. Drucker, D.J. Glucagon-like peptides: regulators of cell proliferation, differentiation, and apoptosis. *Mol. Endocrinol.* **17**, 161–171 (2003).
11. Fredriksson, R., *et al.* Seven evolutionarily conserved human rhodopsin G protein-coupled receptors lacking close relatives. *FEBS Lett.* **554**, 381–388 (2003).
12. Tsao, P., Cao, T. & von Zastrow, M. Role of endocytosis in mediating downregulation of G-protein-coupled receptors. *Trends. Pharmacol. Sci.* **22**, 91–96 (2001).
13. Ding, G.J., *et al.* Characterlization and quantitation of NF-κB nuclear translocation induced by interleukin-1 and tumor necrosis factor-α. Development and use of a high capacity fluorescence cytometric system. *J. Biol. Chem.* **273**, 28897–28905 (1998).
14. Milligan, G., Marshall, F. & Rees, S. G16 as a universal G protein adapter: implications for agonist screening strategies. *Trends. Pharmacol. Sci.* **17**, 235–237 (1996).
15. Vilsboll, T., *et al.* Incretin secretion in relation to meal size and body weight in healthy subjects and people with type 1 and type 2 diabetes mellitus. *J. Clin. Endocrinol. Metab.* **88**, 2706–2713. (2003).
16. Holst, J.J. & Orskov, C. Incretin hormones--an update. *Scand. J. Clin. Lab. Invest.* Suppl.**234**, 75–85 (2001).
17. Guimbaud, R., *et al.* Intraduodenal free fatty acids rather than triglycerides are responsible for the release of CCK in humans. *Pancreas* **14**, 76–82 (1997).
18. Sidhu, S.S., Thompson, D.G., Warhurst, G., Case, R.M. & Benson, R.S. Fatty acid-induced cholecystokinin secretion and changes in intracellular Ca^{2+} in two enteroendocrine cell lines, STC-1 and GLUTag. *J. Physiol.* **528**, 165–176 (2000).
19. Itoh, Y., *et al.* Free fatty acids regulate insulin secretion from pancreatic beta cells through GPR40. *Nature* **422**, 173–176 (2003).
20. Cao, X., *et al.* Aberrant regulation of human intestinal proglucagon gene expression in the NCI-H716 cell line. *Endocrinology* **144**, 2025–2033 (2003).
21. Reimer, R.A., *et al.* A human cellular model for studying the regulation of glucagon-like peptide-1 secretion. *Endocrinology* **142**, 4522–4528 (2001).
22. Trogan, E., *et al.* Laser capture microdissection analysis of gene expression in macrophages from atherosclerotic lesions of apolipoprotein E-deficient mice. *Proc. Natl. Acad. Sci. USA* **99**, 2234–2239 (2002).
23. Briscoe, C.P., *et al.* The orphan G protein-coupled receptor GPR40 is activated by medium and long chain fatty acids. *J. Biol. Chem.* **278**, 11303–11311 (2003).
24. Brown, A.J., *et al.* The Orphan G protein-coupled receptors GPR41 and GPR43 are activated by propionate and other short chain carboxylic acids. *J. Biol. Chem.* **278**, 11312–11319 (2003).
25. Nilsson, N.E., Kotarsky, K., Owman, C. & Olde, B. Identification of a free fatty acid receptor, FFA2R, expressed on leukocytes and activated by short-chain fatty acids. *Biochem. Biophys. Res. Commun.* **303**, 1047–1052 (2003).
26. Hirasawa, A., *et al.* Subtype-specific differences in subcellular localization of α1-adrenoceptors: chlorethylclonidine preferentially alkylates the accessible cell surface α1-adrenoceptors irrespective of the subtype. *Mol. Pharmacol.* **52**, 764–770 (1997)
27. Awaji, T., *et al.* Real-time optical monitoring of ligand-mediated internalization of alpha1b-adrenoceptor with green fluorescent protein. *Mol. Endocrinol.* **12**, 1099–1111 (1998).
28. Horie, K., Hirasawa, A. & Tsujimoto, G. The pharmacological profile of cloned and stably expressed alpha 1b-adrenoceptor in CHO cells. *Eur. J. Pharmacol.* **268**, 399–407 (1994).
29. Awaji, T., Hirasawa, A., Shirakawa, H., Tsujimoto, G., Miyazaki, S. Novel green fluorescent protein-based ratiometric indicators for monitoring pH in defined intracellular microdomains. *Biochem. Biophys. Res. Commun.* **289**, 457–462 (2001).
30. Gevrey, J.C., Cordier-Bussat, M., Nemoz-Gaillard, E., Chayvialle, J.A. & Abello, J. Co-requirement of cyclic AMP- and calcium-dependent protein kinases for transcriptional activation of cholecystokinin gene by protein hydrolysates. *J. Biol. Chem.* **277**, 22407–22413 (2002).

Table 1 pEC_{50}s of fatty acids tested on HEK 293 cells stably expressing GPR120-Gα16

Fatty acid	pEC50 ± s.e.m
n-Caproic acid (C6)	inactive
Octanoic acid (C8)	inactive
Nonanoic acid (C9)	inactive
n-Capric acid (C10)	inactive
Lauric acid (C12)	inactive
Myristic acid (C14)	4.53 ± 0.17
Palmitic acid (C16)	4.28 ± 0.1
Palmitoleic acid (C16:1)	5.49 ± 0.17
Stearic acid (C18)	4.74 ± 0.12
Elaidic acid (C18:1)	4.48 ± 0.23
Oleic acid (C18:1)	4.51 ± 0.19
α-Linolenic acid (C18:3)	6.37 ± 0.13
α-Linolenic acid methyl ester	inactive
γ-Linolenic acid (C18:3)	5.98 ± 0.12
Arachidic acid (C20)	inactive
cis-8,11,14-Eicosatrienoic acid (C20:3)	4.84 ± 0.03
cis-11,14,17-Eicosatrienoic acid (C20:3)	5.85 ± 0.03
cis-5,8,11,14,17-Eicosapentaenoic acid (C20:5)	5.55 ± 0.03
Behenic acid (C22)	inactive
cis-13,16,19-Docosatrienoic acid (C22:3)	inactive
cis-7,10,13,16-Docosatetraenoic acid (C22:4)	4.79 ± 0.11
cis-7,10,13,16,19-Docosapentaenoic acid (C22:5)	4.58 ± 0.22
cis-4,7,10,13,16,19-Docosahexaenoic acid (DHA, C22:6)	5.41 ± 0.11

Receptor activation was measured from dose-dependent changes in $[Ca^{2+}]_i$ levels using a fluorometric imaging plate reader. Inactive, no response at 100 μM.

Ca^{2+} influx-mediated histamine synthesis and IL-6 release in mast cells activated by monomeric IgE

Satoshi Tanaka, Sonoko Mikura, Eri Hashimoto, Yukihiko Sugimoto and Atsushi Ichikawa

Department of Physiological Chemistry, Graduate School of Pharmaceutical Sciences, Kyoto University, Kyoto, Japan

Received 31/8/04
Accepted 14/12/04

[DOI 10.1002/eji.200425622]

We previously demonstrated that histamine synthesis is drastically induced upon sensitization with an anti-DNP IgE clone, SPE-7, in IL-3-dependent mouse bone marrow derived mast cells (BMMC). We found that Ca^{2+} mobilization induced by SPE-7 exhibited a similar profile to the capacitative Ca^{2+} entry evoked by thapsigargin. Potentials for activation of mast cells were found to vary between different IgE clones, and a monovalent hapten, DNP-lysine, suppressed the activation induced by SPE-7. Ca^{2+} mobilization induced by SPE-7 was suppressed potently by the specific store-operated Ca^{2+} channel inhibitor, SK&F 96365, but not at all by Ca^{2+} channel inhibitors with more broad spectrum, La^{3+} and Gd^{3+}, whereas the Ca^{2+} mobilization induced by Ag stimulation was suppressed by these inhibitors. Ca^{2+} mobilization was also induced by SPE-7 in *in vitro* differentiated mast cells, although the increases in histamine synthesis and IL-6 release were smaller than those in BMMC. These results suggest that Ca^{2+} influx operated by a distinct mechanism from that in Ag stimulation is essential for increased histamine synthesis and IL-6 release in mast cells.

Key words: Mast cell · IgE · Ca^{2+} influx · IL-6 · Histamine

Introduction

Activation of mast cells triggers allergic and inflammatory responses through the release of a wide variety of mediators, such as histamine, arachidonic acid metabolites, and neutral proteases, and regulates immune responses through the production of cytokines and chemokines [1, 2]. Recent studies have suggested that, in addition to allergy mast cells are also involved in autoimmunity [3]. One of the major mechanisms for the stimulation of mast cells is cross-linking of the FcεRI, the high-affinity receptor for IgE, by the multivalent Ag, and a variety of signaling molecules have been identified in this pathway [4, 5]. Furthermore, accumulating evidence has indicated that IgE-mediated activation of mast cells can occur even in the absence of the multivalent Ag. Sensitization of IL-3-dependent mouse bone marrow-derived mast cells (BMMC) with IgE induces an array of events, such as the up-regulation of the FcεRI [6, 7], survival under IL-3 depletion [8–10], cytokine production [9, 10], histamine synthesis [11], and adhesion to fibronectin [12] in the absence of Ag stimulation. These results have clearly indicated that sensitization with IgE is able to change a number of characteristics of BMMC. Regarding the IgE-mediated activation of mast cells, weak Ag stimulation, which was induced at lower Ag concentrations or at lower receptor occupancy with IgE, was recently found to cause the production of an array of pro-inflammatory cytokine/chemokines with minimal degranulation in BMMC [13]. These results indicate that mediator release and degranulation of mast cells is finely tuned through IgE-mediated activation of the FcεRI. However, it remains to be clarified as to how monomeric IgE activates mast cells and what kinds of signaling molecules are involved in this pathway.

Correspondence: Atsushi Ichikawa, School of Pharmaceutical Sciences, Mukogawa Women's University, Koshien, Nishinomiya, Hyogo 663–8179, Japan
Fax: +81–798–41–2792
e-mail: aichikaw@mwu.mukogawa-u.ac.jp

Abbreviations: $[Ca^{2+}]_i$: Cytosolic Ca^{2+} concentration · **BMMC:** Bone marrow-derived mast cells · **HDC:** Histidine decarboxylase · **SHIP:** Src homology 2-containing inositol phosphatase · **CTMC:** Connective tissue-type mast cell

We found in a previous study that a monomeric IgE, SPE-7 is able to induce histidine decarboxylase (HDC), which is completely abolished by depletion of the extracellular Ca^{2+}, indicating the essential role of Ca^{2+} influx in this induction [11]. SPE-7-mediated Ca^{2+} influx has been previously reported in BMMC [14], where the stimulation with monomeric IgE was found to trigger degranulation in the absence of the Src homology 2-containing inositol phosphatase (SHIP). This result suggests that a large part of the signaling pathway may be shared between monomeric IgE and Ag stimulation, although it remains unknown whether Ca^{2+} influx is activated by the same mechanism between monomeric IgE and Ag stimulation. In the current study, we focused on the mechanism of this Ca^{2+} influx induced by monomeric IgE, and found that Ca^{2+} influx upon stimulation with monomeric IgE is induced by a different system from that upon Ag stimulation. Furthermore, we investigated whether monomeric IgE-mediated activation of mast cells could occur in mature mast cells, since previous studies have demonstrated the effects of monomeric IgE mainly using BMMC, which is generally regarded as a model of immature mast cells.

Results

Ca^{2+}-influx-mediated induction of HDC and IL-6 in BMMC stimulated with monomeric IgE

We previously demonstrated that histamine synthesis in BMMC is induced by monomeric IgE in extracellular Ca^{2+}-dependent manner [11]. However, Ca^{2+} mobilization, especially Ca^{2+} influx, induced by monomeric IgE has not been investigated in detail. We focused on the role of Ca^{2+} influx in the induction of HDC in BMMC sensitized with IgE. Treatment of BMMC with IgE (anti-DNP IgE, SPE-7) or with thapsigargin, a sarco/endoplasmic Ca^{2+}-ATPase inhibitor, drastically induced HDC mRNA expression and IL-6 release, both of which were completely abolished in the absence of extracellular Ca^{2+} (Fig. 1A). In the absence of extracellular Ca^{2+}, addition of SPE-7 induced a transient increase in cytosolic Ca^{2+} concentration ($[Ca^{2+}]_i$), to a level similar to that induced by thapsigargin (Fig. 1B, left panels). This transient increase in $[Ca^{2+}]_i$ by SPE-7 was not detected in BMMC pretreated with thapsigargin (Fig. 1B, right panels). These results indicate that SPE-7 triggers Ca^{2+} release from intracellular thapsigargin-sensitive stores in the absence of extracellular Ca^{2+}. Furthermore, addition of Ca^{2+} to the extracellular milieu caused a rapid and large increase in $[Ca^{2+}]_i$ in BMMC sensitized with SPE-7, and the profile of this increase was similar to the capacitative Ca^{2+} entry induced by thapsigargin (Fig. 1B, left panels).

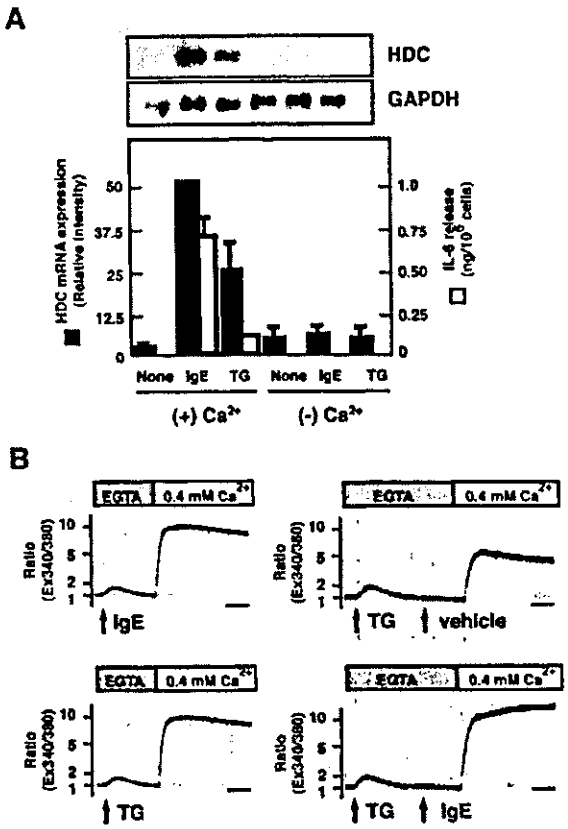

Fig. 1. Requirement of extracellular Ca^{2+} for IgE-mediated induction of HDC and IL-6 in BMMC. (A) BMMC were incubated in PIPES buffer with [(+)Ca^{2+}] or without [(–)Ca^{2+}] Ca^{2+} for 90 min in the presence of an IgE clone, SPE-7 (IgE, 3 μg/ml) or thapsigargin (TG, 0.1 μM). The cells were then harvested and Northern blot analyses were performed. The relative intensities of the bands hybridized with the probe for HDC were normalized by those with the probe for GAPDH. The medium was also simultaneously collected at the time of cell harvest and subjected to an ELISA assay for IL-6. The values are represented as the means ± SEM (n=3). (B) Ca^{2+} influx induced by SPE7 was compared with that induced by thapsigargin. BMMC were loaded with 2 μM Fura-2/AM in modified Tyrode's buffer as described in the Materials and methods. SPE7 (IgE, 10 μg/ml) or thapsigargin (TG, 0.1 μM) was added to the cells in the buffer without Ca^{2+} at the time point indicated by the arrows. Ca^{2+} influx was detected by the addition of $CaCl_2$ to the buffer. Bars=2 min. This is a representative figure of three independent experiments showing similar results.

Activation of BMMC induced by different IgE clones

Kitaura et al. [10] previously reported that different IgE clones induce different responses in IL-6 release from BMMC. We addressed the question whether this difference is also observed in HDC induction and Ca^{2+} mobilization. Flowcytometric analysis demonstrated that two anti-TNP IgE clones, clone IgE-3, and

c38–2, bound to BMMC at similar levels to that of SPE-7 (Fig. 2A). Although c38–2 was found to induce $[Ca^{2+}]_i$ increase in BMMC as well as SPE-7, IgE-3 did not change $[Ca^{2+}]_i$ (Fig. 2B). Furthermore, IgE-3 had no inducible effect on HDC expression and IL-6 release in BMMC (Fig. 2C). The other anti-TNP IgE clone, c38–2, was found to significantly induce both HDC activity and IL-6 release, although the levels were lower than that induced by SPE-7. Analysis of the concentration dependency revealed that higher concentrations (up to 30 μg/ml) of IgE-3 or c38–2 did not further augment HDC activity nor IL-6 release (data not shown).

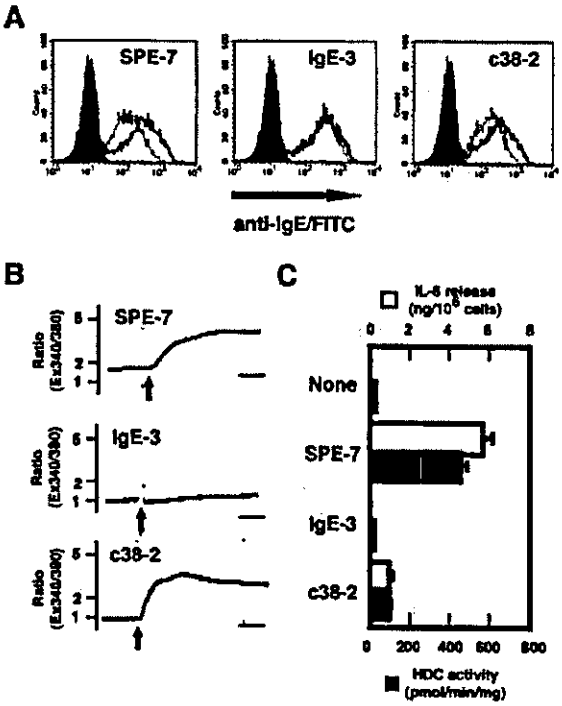

Fig. 2. Effects of different IgE clones on intracellular Ca^{2+} mobilization and induction of HDC and IL-6 in BMMC. (A) Surface binding of three IgE clones (SPE-7, IgE-3, and c38–2) to BMMC was measured by flow cytometry. BMMC were incubated with 3 μg/ml (dashed lines) or 12.5 μg/ml (solid lines) of each IgE clone for 50 min at 4°C, followed by the labeling with an FITC-conjugated anti-mouse IgE. The left closed area profiles were obtained with isotype control antibodies. (B) Intracellular Ca^{2+} mobilization was measured using Fura-2/AM. BMMC were stimulated with each IgE clone (10 μg/ml) in modified Tyrode's buffer containing 1.4 mM $CaCl_2$ at the time point indicated by the arrows. Bars=1 min. This is a representative figure of three independent experiments showing similar results. (C) BMMC were incubated with each IgE clone (3 μg/ml) for 3 h to measure IL-6 release (IL-6) or for 6 h to measure HDC activity (HDC). Concentration of each IgE clone was determined in preliminary experiments to obtain maximal effect. The values are represented as the means ± SEM (n=3). No detectable release of IL-6 was observed in untreated BMMC (None) and BMMC treated with IgE-3.

Inhibition by monovalent hapten of IgE-mediated Ca^{2+} mobilization, HDC induction, and IL-6 release in BMMC

It has been reported that activation of mast cells upon cross-linking of the FcεRI by the multivalent Ag via an anti-DNP IgE can be suppressed by adding an excess amount of a monovalent hapten, DNP-lysine [15]. Addition of DNP-lysine suppressed increases in $[Ca^{2+}]_i$, which was induced not only by Ag stimulation (Fig. 3A, right panels), but also by SPE-7 (Fig. 3A, left panels). Addition of DNP-lysine did not change the increase in $[Ca^{2+}]_i$ induced by c38–2 (data not shown). Increases in HDC activity and IL 6 release induced by SPE-7 were largely abolished by DNP-lysine treatment both before and after addition of SPE-7 (Fig. 3B).

Effects of various Ca^{2+} channel blockers on IgE-induced intracellular Ca^{2+} mobilization

The similarity of intracellular Ca^{2+} mobilization induced between by monomeric IgE and by thapsigargin suggests that the elevation of intracellular Ca^{2+} levels are maintained through the capacitative Ca^{2+} entry. We first investigated the effects of an array of store-operated Ca^{2+} channel (SOC) inhibitors, such as La^{3+}, Gd^{3+}, and SK&F 96365 [16], to characterize this Ca^{2+} entry. These inhibitors completely abolished the capacitative Ca^{2+} entry induced by thapsigargin in BMMC at the concentrations used in this study (data not shown). However, La^{3+} and Gd^{3+}, had no effect on the intracellular Ca^{2+} mobilization induced by SPE-7, although both cations significantly suppressed the increase in $[Ca^{2+}]_i$ by Ag stimulation, especially in its sustained phase, even at lower concentrations (Fig. 4). The inhibitory effects of La^{3+} on the mRNA expression of HDC were found to be significant upon Ag stimulation but not upon monomeric IgE stimulation; monomeric IgE stimulation, 18.4±6.64 (None) *vs.* 14.1±5.56 (+La^{3+}, 100 μM), Ag stimulation, 5.68±2.17 (None) *vs.* 1.12±0.379* (+La^{3+}, 100 μM) (45 min incubation, fold increase, n=3, *p<0.05 by the Student's t-test). On the other hand, pretreatment with SK&F 96365, suppressed the increases in $[Ca^{2+}]_i$ induced by both SPE-7 and Ag stimulation. We could not investigate the effects of Gd^{3+} and SK&F 96365 on the HDC mRNA expression due to the impaired viability of the cells upon prolonged treatment.

Effects of protein kinase/phosphatase inhibitors on monomeric IgE-induced Ca^{2+} mobilization

We next examined the effects of an array of protein kinase/phosphatase inhibitors on monomeric IgE-in-

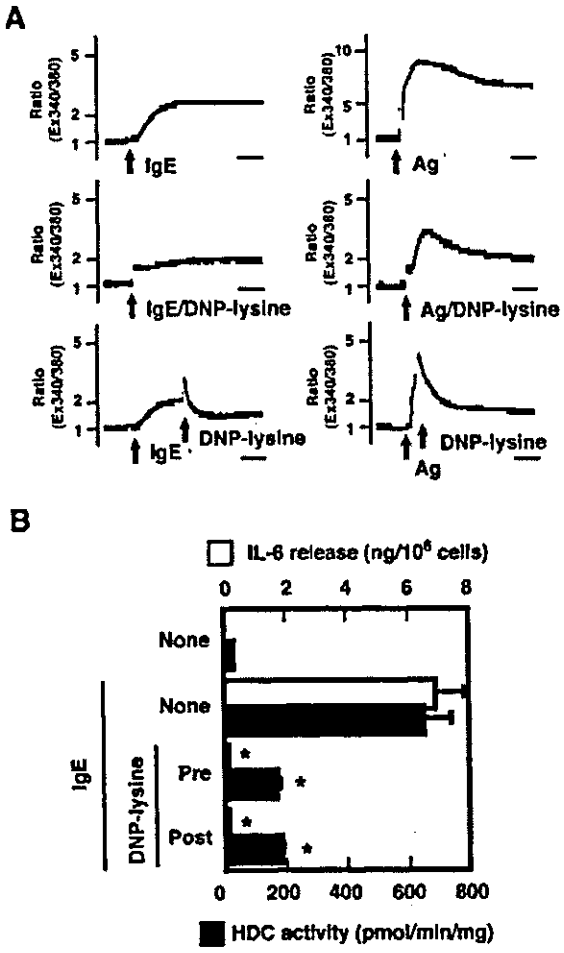

Fig. 3. Inhibition of IgE-mediated Ca^{2+} mobilization and induction of HDC and IL 6 by a monovalent hapten in BMMC. (A) Effects of a monovalent hapten, DNP-lysine, on intracellular Ca^{2+} mobilization induced by SPE-7 (10 μg/ml, left, IgE) or by Ag stimulation (right, Ag) were investigated. In the Ag stimulation experiment, BMMC were sensitized with SPE-7 (1 μg/ml) 12 h before the stimulation (Ag, 30 ng/ml DNP-HSA). DNP-lysine (final concentration, 10 μg/ml) was added to BMMC after preincubation for 10 min at 37°C with SPE-7 (IgE/DNP-lysine) or with DNP-HSA (Ag/DNP-lysine) (middle panels), or after the stimulation of BMMC with SPE-7 or DNP-HSA (lower panels). The time points of addition of SPE-7 (IgE), DNP-HSA (Ag), and DNP-lysine are indicated by the arrows. Bars=1 min. This is a representative figure of three independent experiments showing similar results. (B) Induction of HDC and IL-6 by SPE-7 (IgE, 3 μg/ml) was measured as described in the legend to Fig. 2 in the presence or absence of DNP-lysine (10 μg/ml). DNP-lysine was added after preincubation with SPE-7 (Pre) or 10 min after the addition of SPE-7 to BMMC (Post). The values are represented as the means ± SEM (n=3). The values of $^*p<0.05$ (vs. IgE/None) are regarded as significant by the Student's t-test.

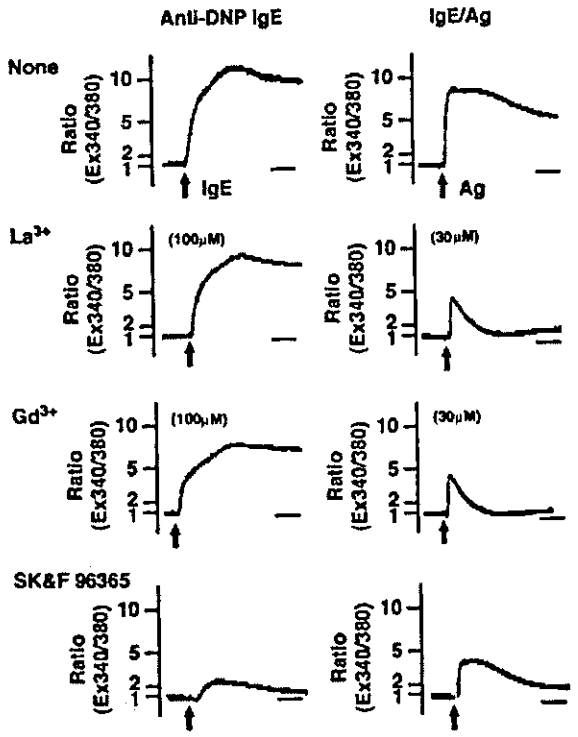

Fig. 4. Effects of SOC inhibitors on IgE-mediated Ca^{2+} mobilization in BMMC. (A) Intracellular Ca^{2+} mobilization in the presence of various SOC inhibitors was measured using Fura-2/AM. BMMC were stimulated with SPE-7 (10 μg/ml) in modified Tyrode's buffer containing 1.4 mM $CaCl_2$ at the time points indicated by the arrows (Anti-DNP IgE, left). In the Ag stimulation experiment, BMMC were sensitized with SPE-7 (1 μg/ml) 12 h before Ag stimulation (Ag, 30 ng/ml DNP-HSA, right). The cells were pretreated with the following SOC inhibitors; La^{3+}, 30 or 100 μM, 3 min, Gd^{3+}, 30 or 100 μM, 3 min, SK&F 96365, 100 μM, 3 min. Bars=1 min. This is a representative figure of three independent experiments showing similar results.

duced changes, such as intracellular Ca^{2+} mobilization, HDC induction, and IL-6 release. Although involvement of various kinases in activation of mast cells has been demonstrated, it remains to be determined what kinds of kinases are involved in the monomeric IgE-induced Ca^{2+} mobilization. Staurosporine, Gö6976, piceatannol, and cyclosporin A were able to suppress the induction of both HDC activity and IL-6 release (Fig. 5A). Staurosporine, Gö6976, and piceatannol demonstrated potent inhibitory effects on the increase in $[Ca^{2+}]_i$ induced by SPE-7, whereas cyclosporin A did not (Fig. 5B).

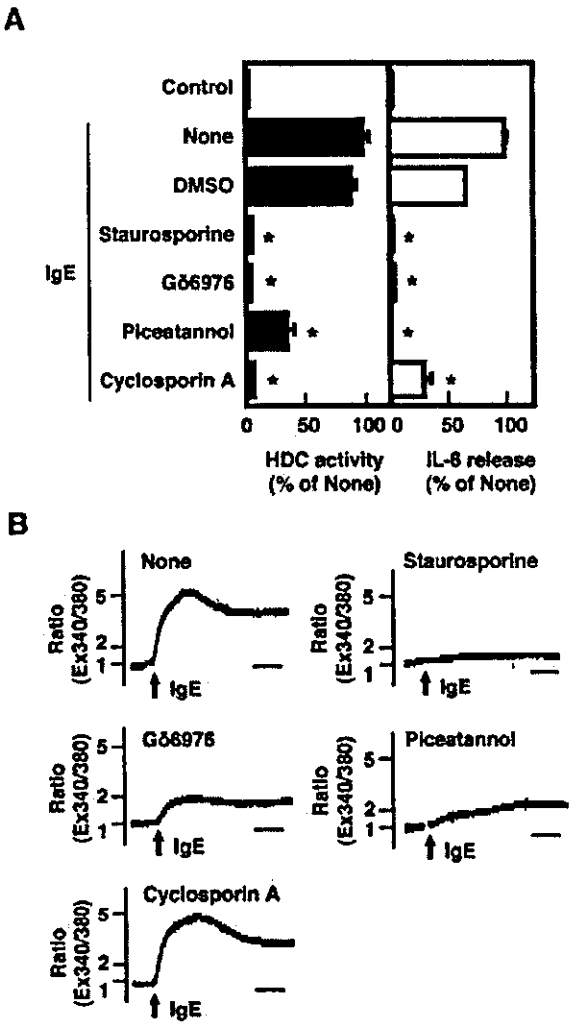

Fig. 5. Inhibition of IgE-mediated Ca^{2+} mobilization and induction of HDC and IL-6 by various kinase inhibitors in BMMC. (A) BMMC were pretreated with staurosporine (1 μM, 10 min), Gö6976 (10 μM, 60 min), piceatannol (30 μg/ml, 60 min), or cyclosporin A (10 μM, 15 min). The cells were then incubated with 3 μg/ml SPE-7 (IgE) for 6 h at 37°C, and HDC activity and IL-6 release were measured. The values are represented as the means ± SEM (n=3). The values of $^*p<0.05$ (*vs.* DMSO) are regarded as significant by the Student's t-test. (B) BMMC were pretreated with various inhibitors as described above and intracellular Ca^{2+} mobilization induced by SPE-7 (IgE, 10 μg/ml) was measured as described in the legend to Fig. 2. Bars=1 min. This is a representative figure of three independent experiments showing similar results.

Effects of monomeric IgE on induction of histamine synthesis in rat peritoneal mast cells

We then investigated the effects of monomeric IgE on histamine synthesis using peritoneal mast cells in place of BMMC to confirm the responses to monomeric IgE in mature mast cells. Since it was quite difficult to obtain enough amounts of mouse peritoneal mast cells to determine the enzymatic activity of HDC, we performed the experiments using rat peritoneal mast cells. Treatment of rat peritoneal mast cells with SPE-7 caused both a transient increase in $[Ca^{2+}]_i$ and a significant increase in HDC activity (Fig. 6). A transient increase in $[Ca^{2+}]_i$ was also observed in mouse peritoneal mast cells (data not shown). Furthermore, this inducible effect of SPE-7 on HDC was not observed in the presence of stem cell factor (SCF), whereas SCF alone could also augment HDC activity in the peritoneal mast cells by 2.5-fold (Fig. 6).

Effects of monomeric IgE on connective tissue-type mast cell (CTMC)-like cultured mast cells differentiated *in vitro*

The induction levels of HDC activity observed in peritoneal mast cells stimulated with SPE-7 (about 2-fold) were much lower than those observed in BMMC (about 200-fold). Given that sensitivity to monomeric IgE are similar in mast cells derived from between rats and mice, this result raises the possibility that differentiation of mast cells toward connective tissue-

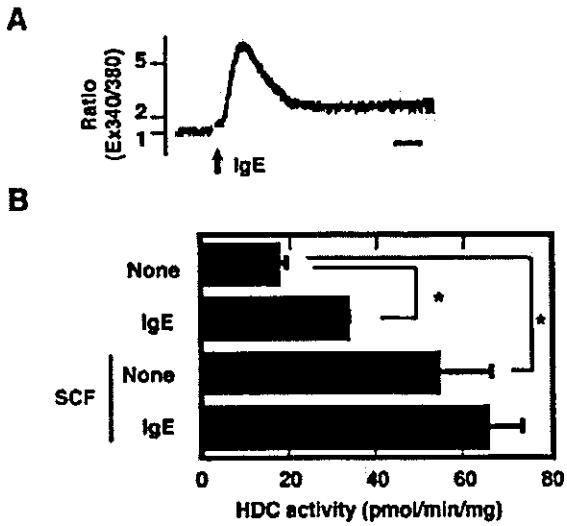

Fig. 6. Increased histamine synthesis upon sensitization with IgE *in vivo*. (A) Peritoneal mast cells were purified from the peritoneal cavity of male Wistar rats by density gradient fractionation. Intracellular Ca^{2+} mobilization was measured using Fura-2/AM as described in the legend to Fig. 2 (upper panel). The arrow indicates the time point of addition of SPE-7 (IgE, 10 μg/ml). Bars=1 min. This is a representative figure of three independent experiments showing similar results. (B) Peritoneal mast cells were incubated for 6 h with (IgE) or without (None) SPE-7 (3 μg/ml) in the presence or absence of SCF (SCF, 100 ng/ml) and HDC activity was measured. The values are represented as the means ± SEM (n=3). The values of $^*p<0.05$ are regarded as significant by the Student's t-test.

type mast cell (CTMC) is accompanied by decreased sensitivity to monomeric IgE. We verified this hypothesis using CTMC-like cultured mast cells, which were derived from BMMC by coculturing with Swiss 3T3 fibroblasts for 16 days in the presence of SCF. Treatment of these CTMC-like cultured cells with SPE-7 caused a transient increase in $[Ca^{2+}]_i$ and a smaller but significant increase in HDC activity (about 5-fold, Fig. 7A and B). Thapsigargin was also found to augment HDC activity to a similar extent to that by SPE-7. These increases in HDC activity by SPE-7 and thapsigargin were accompanied by an increase in HDC mRNA, indicating induction at the transcriptional level (Fig. 7C). A significant amount of IL-6 release was also detected upon treatment with SPE-7 or thapsigargin, but was smaller than that released from BMMC (Fig. 7B, compared with Figs. 2 and 3).

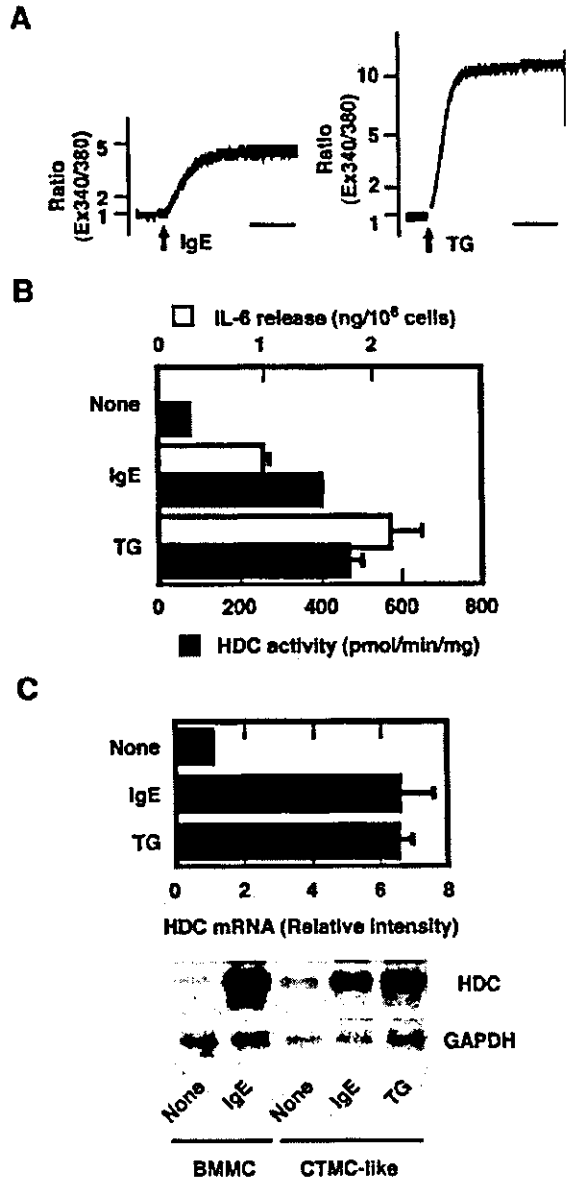

Fig. 7. Induction of intracellular Ca^{2+} mobilization, HDC, and IL-6 by IgE in CTMC-like cultured cells. (A) CTMC-like cultured mast cells were prepared as described in the Materials and methods. Intracellular Ca^{2+} mobilization was measured using Fura-2/AM as described in the legend to Fig. 2. The arrow indicates the time point of addition of SPE-7 (IgE, 10 μg/ml) or thapsigargin (TG, 0.1 μM). Bars=1 min. This is a representative figure of three independent experiments showing similar results. (B) CTMC-like mast cells were incubated for 3 h to measure IL-6 release (IL-6) or 6 h to measure HDC activity (HDC) with SPE-7 (IgE, 3 μg/ml) or thapsigargin (TG, 0.1 μM) in the presence of SCF (100 ng/ml). IL-6 release and HDC activity were then measured. The values are represented as the means ± SEM (n=3). (C) CTMC-like mast cells were incubated for 3 h with SPE-7 (IgE, 3 μg/ml) or thapsigargin (TG, 0.1 μM) in the presence of SCF (100 ng/ml). The cells were then harvested and Northern blot analyses were performed. The relative intensities of the bands hybridized with the probe for HDC were normalized by those with the probe for GAPDH. The values are represented as the means ± SEM (n=3). A representative result is shown (lower panel, CTMC-like) in comparison with BMMC.

Discussion

We focused on the intracellular Ca^{2+} mobilization upon sensitization with IgE in BMMC and found a close correlation between the Ca^{2+} mobilization and induction of HDC or IL-6. Intracellular Ca^{2+} mobilization in BMMC sensitized with IgE, which was first demonstrated by Huber et al. [14], has not been characterized in detail. We demonstrated that Ca^{2+} mobilization induced by monomeric IgE shares some similarities with thapsigargin-induced capacitative Ca^{2+} entry. Calcium release-activated Ca^{2+} (CRAC) channels in mast cells, which are activated by Ag stimulation, are one of the best characterized store-operated Ca^{2+} channels (SOC) [17–19]. Indeed, an array of SOC inhibitors, such as La^{3+}, and SK&F 96365, have been reported to inhibit the CRAC current, I_{CRAC}, evoked by Ag stimulation in a rat mast cell line, RBL-2H3 [20, 21]. We observed similar results with these inhibitors as well as Gd^{3+}, which was also found to inhibit I_{CRAC} [22] and have suppressive effects on Ca^{2+} mobilization in BMMC stimulated with Ag. On the other hand, Ca^{2+} mobilization induced by monomeric IgE was suppressed by SK&F 96365, but not at all by La^{3+} and Gd^{3+}. This difference suggests that IgE-induced Ca^{2+} influx is mediated by a distinct mechanism from that operating during Ag stimulation. Accumulating evidence has suggested that mammalian homologs of transient receptor potential (TRP), such as TRPC1, TRPC3, TRPC4, and TRPV6 (CaT1), are potent

candidates of SOC, although the molecular identity of SOC still remains controversial [18, 19]. It is quite difficult to approach the molecular identity of the Ca^{2+} channel involved in activation of BMMC sensitized with IgE, since a Ca^{2+} channel that is sensitive to SK&F 96365, but not to La^{3+} and Gd^{3+}, has not been previously described and the TRP family has been reported to form heteromultimers *in vitro* and *in vivo*, in some cases generating altered pore properties [23, 24].

We previously demonstrated that various kinase inhibitors for protein kinase C (PKC) and tyrosine kinases are able to suppress histamine synthesis induced by IgE in BMMC [11]. These inhibitors were found to suppress IL-6 release from BMMC sensitized with IgE in addition to HDC activity. PKC may be involved in the regulation of Ca^{2+} influx, since the $[Ca^{2+}]_i$ increase induced by IgE was suppressed by staurosporine and Gö6976. A specific inhibitor for Syk, piceatannol, was found to inhibit activation of BMMC completely, which is consistent with the results obtained using the Syk-deficient mice [10]. The inhibitory effects of cyclosporin A suggest that activation of NFAT is required for histamine synthesis and IL-6 production, which is consistent with the result that Ca^{2+} influx is essential for induction of HDC and IL-6, since activation of NFAT requires prolonged $[Ca^{2+}]_i$ elevation in immune cells [25]. Very recently, Pandy et al. [26] demonstrated the induction of the nuclear translocation of NFAT in RBL-2H3 cells by monomeric IgE.

We evaluated the activation of BMMC by IgE using three indexes, Ca^{2+} mobilization, HDC activity, and IL-6 release. Three different IgE clones tested in this study demonstrated different potentials for activation, although they displayed equal levels of binding to the surface of BMMC. Furthermore, the activation of BMMC by IgE was completely suppressed by its monovalent hapten. Regarding IL-6 production, identical results have previously been demonstrated by Kitaura et al. [10]. They also demonstrated that the monovalent hapten abolished the anti-apoptic effects induced by IgE (SPE-7) and suppressed the phosphorylation of Akt, extracellular signal-regulated protein kinase (ERK), and p38 MAPK (mitogen-activated protein kinase) [10]. These results suggest that a certain conformation of IgE including its Ag binding sites are required for the activation of BMMC by IgE, and that the monovalent hapten may disturb the formation of this conformation by binding to the IgE. We furthermore investigated the homomeric interaction of the SPE-7 molecule by the surface plasmon resonance experiments using the BIAcore 3000 system (BIAcore, Uppsala, Sweden), but failed to detect a significant level of interaction between these IgE molecules (data not shown). James et al. [27] recently demonstrated that SPE-7, which has been found to exert the most potent effects on mast cells in the absence of Ag among the various IgE clones tested ([10] and in this study), adopts at least two different pre-existing conformations that are independent of the Ag, each conferring a different Ag-binding function. This result indicates the structural flexibility of the IgE molecule. A time-resolved phosphorescence anisotropy study suggested the aggregation of the IgE molecules on the surface of the rat mast cell line, RBL-2H3, in the absence of Ag [10], although its mechanism remains to be clarified. These results raise the possibility that a certain IgE molecule may have a potential to interact with each other only after binding to the surface FcεRI. However, further experimental approaches are required to verify this hypothesis.

Mouse models of IgE depletion have indicated that serum IgE plays important roles in regulation not only of FcεRI expression in mast cells but also of allergic responses, such as eosinophil infiltration and bronchial hyper reactivity [7, 28]. Monomeric IgE was also found to induce Ca^{2+} mobilization and augment histamine synthesis both in rat peritoneal mast cells and in CTMC-like cultured mast cells, although the effects of monomeric IgE in these cells were all smaller than those observed in BMMC. Lam et al. [12] have also demonstrated that monomeric IgE (SPE-7) augments adhesion of both BMMC and CTMC-like cells to fibronectin. Interestingly, the IgE-induced enhancement of adhesion of CTMC-like cells was less than that of BMMC and basal adhesion was increased in CTMC-like cells. The increases in histamine synthesis and IL-6 release induced by IgE were also less in CTMC-like cells compared with BMMC. These results suggest that elevated serum IgE levels could lead to the altered characteristics of tissue mast cells, especially of immature mast cells. We preliminary investigated the effect of SPE-7 on HDC activity in skin tissues of mouse ears. SPE-7 was found to cause about twofold increase in the tissue HDC activity 6 h after the intradermal injection (data not shown). We could not detect any changes in number and morphology of the tissue mast cells and did not find the other candidates for histamine-forming cells, such as infiltrated neutrophils [29] and macrophages [30]. This observation is consistent with the results obtained using peritoneal mast cells and suggests that IgE has the potential to augment histamine synthesis *in vivo*. Very recently, Bryce et al. [31] demonstrated through the excellent study using the IgE-deficient mice that IgE plays an essential role in the sensitization phase of oxazolone-induced contact hypersensitivity responses in Ag-independent manner. This result indicates that the skin mast cells can respond and be activated by monomeric IgE, which is consistent with our results. It surely requires further *in vivo* studies to clarify the roles of monomeric IgE in allergic responses.

In summary, we demonstrated in this study that Ca^{2+} influx operated by a distinct mechanism from that in Ag stimulation is essential for increased histamine synthesis and IL-6 release upon sensitization of BMMC with IgE. Induction of histamine synthesis and IL-6 production by IgE was observed not only in immature cultured mast cells but also in mature cells, although the former seems to be more sensitive to IgE.

Materials and methods

Animals

Specific-pathogen-free, 8-week-old female BALB/c mice and male Wistar rats (250–300 g in weight) were obtained from Japan SLC (Hamamatsu, Japan). All animal experiments were performed according to the Guidelines for Animal Experiments of Kyoto University.

Materials

The following materials were commercially obtained from the sources indicated: an anti-DNP mouse monoclonal IgE (SPE-7), DNP-conjugated human serum albumin, DNP-lysine, H7, and cyclosporin A from Sigma-Aldrich (St. Louis, MO), an anti-TNP mouse monoclonal IgE (IgE-3 and c38–2), an anti-mouse FcγRIIB/III (2.4G2) antibody, and an FITC-conjugated anti-mouse IgE antibody from BD Biosciences (San Diego, CA), staurosporine, Gö6976, PP2, PP3, and piceatannol from Calbiochem (San Diego, CA), SK&F 96365 from TOCRIS (Bristol, UK), stem cell factor (SCF) from Genzyme-Techne (Minneapolis, MN), [α-^{32}P]dCTP (3,000 Ci/mmol) from Du Pont-New England Nuclear (Boston, MA), and Fura-2/AM from Dojindo Laboratories (Kumamoto, Japan). All other chemicals were commercial products of reagent grade.

Preparation of BMMC

BMMC were prepared as described previously [11]. Bone marrow cells were cultured for 4 to 5 weeks in the presence of WEHI-3-conditioned medium as a source of IL-3. Greater than 95% of the viable cells were confirmed to be immature mast cells, as assessed by staining with acidic Toluidine blue.

HDC assay

Preparation of the cell lysate was performed as previously described [11] and HDC activity was measured as previously described in the presence of 0.8 mM L-histidine [32].

Northern blot analyses

Northern blot analyses were performed as previously described [29]. Total RNA (3 μg) was electrophoretically separated on a 1.5% agarose/formaldehyde gel. [α-^{32}P]dCTP-labeled specific cDNA probes for HDC were hybridized. The filter was then analyzed using a Fujix BAS 2000 Bio-Imaging Analyzer.

Measurement of cytosolic Ca^{2+} concentrations

Cytosolic Ca^{2+} concentration was measured as previously described [11]. Fluorescent intensities were measured, at an excitation wavelength of 340 or 380 nm and an emission wavelength of 510 nm, with a fluorescence spectrometer (Jasco, CAF-100, Tokyo, Japan) as described previously [33].

Flow cytometry

BMMC were pretreated with 10 μg/ml 2.4G2 at 4°C for 10 min, then with 3 or 12.5 μg/ml each of the IgE clone at 4°C for 50 min. Labeling of the cells was performed by incubation with an FITC-conjugated anti-mouse IgE at 4°C for 25 min. Flowcytometric analysis of the stained cells was performed with FACSCalibur (Becton Dickinson) equipped with CELL-QUEST software. The dead cell population was gated out by propidium iodide staining.

Treatment with various kinase inhibitors

BMMC were treated for the indicated periods with various kinase inhibitors at the concentrations indicated, before the addition of IgE: a kinase inhibitor with a broad spectrum; Staurosporine (10 min, 1 μM), PKC inhibitor; Gö6976 (60 min, 10 μM), Syk inhibitor; piceatannol (60 min, 30 μg/ml), calcineurin inhibitor; cyclosporin A (15 min, 10 μM).

Isolation and culture of rat peritoneal mast cells

Isolation of rat peritoneal mast cells was performed as previously described [34]. Briefly, rat peritoneal cells were collected by 20 ml of Tyrode-Hepes-gelatin (THG) buffer and centrifuged at 45×g for 5 min. The cell suspension was layered onto 12 ml of 60% Percoll/THG solution, and was centrifuged at 45×g for 15 min. The resultant cell pellet was washed with THG buffer and centrifuged at 200×g for 15 min to obtain purified peritoneal mast cells (>98% of purity confirmed by Alcian blue/Safranin-O staining). The purified peritoneal mast cells were incubated under standard culture conditions for 6 h in RPMI-1640 medium containing 10% heat-inactivated fetal bovine serum, 0.1 mM nonessential amino acids, and 50 μM β-mercaptoethanol (complete RPMI) in the presence or absence of 100 ng/ml SCF.

Preparation of connective tissue-type cultured mast cells

A murine fibroblastic cell line, Swiss 3T3, was cultured in complete RPMI medium and treated with mitomycin C (3 μg/ml) for 3 h. The cells were further cultured in the absence of mitomycin C for 3 h. BMMC were added onto these mitomycin C-treated cells and cocultured in the presence of 100 ng/ml SCF for 16 days. Differentiation of BMMC into CTMC-like cells was confirmed by Alcian blue/Safranin-O staining. The CTMC-like cells were then cultured in complete RPMI medium in the presence of 100 ng/ml SCF. Greater than 98% of the cells were identified as FcεRI$^+$/c-kit$^+$ cells by flow cytometry.